Supplementary Information (SI) for Catalysis Science & Technology.
This journal is © The Royal Society of Chemistry 2025

Supporting Information

Catalytic Static Mixers Enable the Continuous Hydrogenation of Cannabidiol and Tetrahydrocannabinol

Stefano Martinuzzi,[a,b] Felipe L. N. da Silva,[b,c] Martin G. Schmid,[d] Kurt Plöschberger,[d] Rodrigo O. M. A. de Souza,[c] Christopher A. Hone,*[a,b] and C. Oliver Kappe*[a,b]

[a] *Center for Continuous Flow Synthesis and Processing, Research Center Pharmaceutical Engineering GmbH and University of Graz, Graz, Austria.*

[b] *Institute of Chemistry, University of Graz, Graz, Austria.*

[c] *BOSS Group - Biocatalysis and Organic Synthesis Group, Chemistry Institute, Federal University of Rio de Janeiro, Rio de Janeiro, Brazil.*

[d] *Institute for Pharmaceutical Sciences, University of Graz, Graz, Austria.*

*E-mail: christopher.hone@rcpe.at; oliver.kappe@uni-graz.at

Table of Contents

1. General Information

1.1. Catalytic Static Mixers

Catalytic static mixers (Precision Catalysts, 316L12F150-A) with the dimensions 11.8 mm x 150 mm were used in the investigation. The CSMs used for the experimental campaign are reported in Table S 1.

Table S 1: Catalytic static mixers used (Note: LR – Long Run).

Entry	CSM	Serial Number	Experimental Note
1	Pd-EP	346001-8-A042	Screening experiments
2	Pd-EP	346001-8-A043	Screening experiments
3	Pd/alumina	346131-8-A007	Screening experiments
4	Pd/alumina	346131-8-A008	Screening experiments
5	Ru/alumina	344131-4-A015	Screening experiments
6	Ru/alumina	344131-4-A017	Screening experiments
7	Pt/alumina	378131-8-A013	Screening experiments
8	Pt/alumina	378131-8-A014	Long run to prepare H2CBD
9	Pt/alumina	378131-8-A015	Long run to prepare H2CBD
10	Pt/alumina	378131-8-A016	Screening experiments
11	Pt/alumina	378131-8-A017	Kinetics with A020 (CSM A)
12	Pt/alumina	378131-8-A018	Long run to prepare H2CBD
13	Pt/alumina	378131-8-A019	Long run to prepare H2CBD
14	Pt/alumina	378131-8-A020	Hydrogenation of limonene Kinetic study (CSM A)
15	Pt/alumina	346131-8-A236	Long run to prepare H4CBD Long run to prepare HHC
16	Pt/alumina	346131-8-A238	Long run to prepare H4CBD Long run to prepare HHC
17	Pt/alumina	346131-8-A240	Long run to prepare H4CBD Kinetic study (CSM B) Long run to prepare HHC
18	Pt/alumina	346131-8-A241	Long run to prepare H4CBD Kinetics with A240 (CSM B) Long run to prepare HHC

1.2. High Field NMR

NMR spectra were obtained by using a Bruker 300 MHz instrument (^{1}H: 300 MHz, ^{13}C: 75 MHz). All the samples were prepared in acetonitrile-d_3. The chemical shifts of ^{1}H and ^{13}C are given in ppm, relative to the peak of the solvent. Coupling constants are given in Hertz (Hz). Multiplicity is indicated with the following abbreviations: s-singlet, d-doublet, t-triplet, q-quartet and m-multiplet. Carbon and hydrogen spectra are reported at the end of this document from Figure S 39 to Figure S 50.

1.3. GC-FID Analysis

GC-FID analysis was performed by using a Shimadzu GC-FID 230 with a flame ionization detector, suing an RTX-5MS column (30 m x 0.25 mm ID x 0.25 µm) and helium as carrier gas (40 cm/sec linear velocity) and a split ratio of 5. The temperature of the injector was set to 280 °C. After 1 min at 50 °C, the temperature increased by 25 °C/min to 300 °C and kept constant at 300 °C for 4 min. Hydrogen and synthetic air (5.0 quality) were used to ignite the flame of the detector. Examples of chromatograms are provided in Figure S 1 for the processing of CBD and Figure S 2 for the processing of THC.

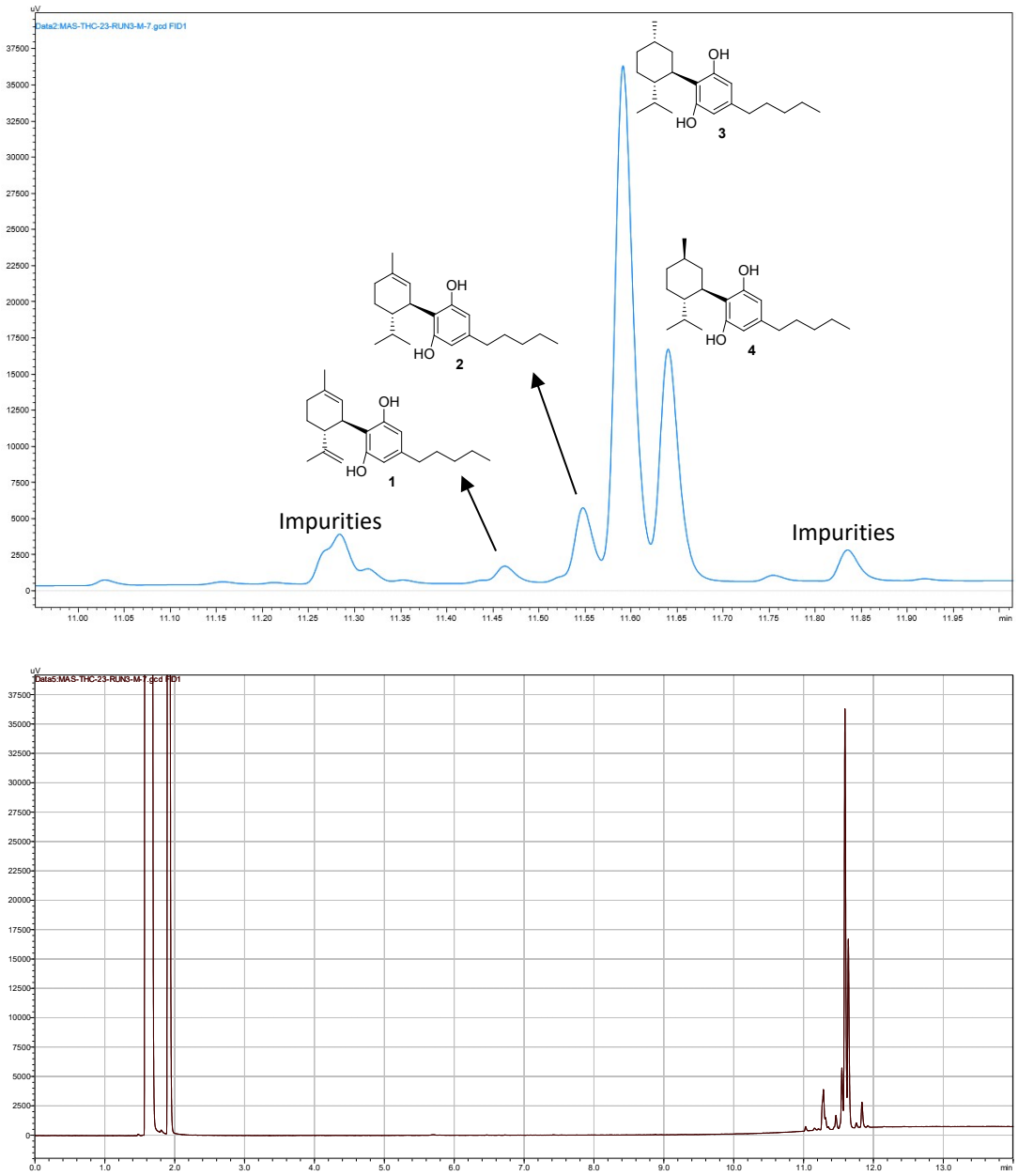

*Figure S 1: Example of GC-FID chromatogram for the hydrogenation of CBD over Pd/alumina CSMs. Retention times: CBD (**1**) (11.46 min); H2CBD (**2**) (11.54 min); cis-H4CBD (**3**) (11.58 min); trans-H4CBD (**4**) (11.64 min). Top – Zoomed in chromatogram; Bottom – Full chromatogram.*

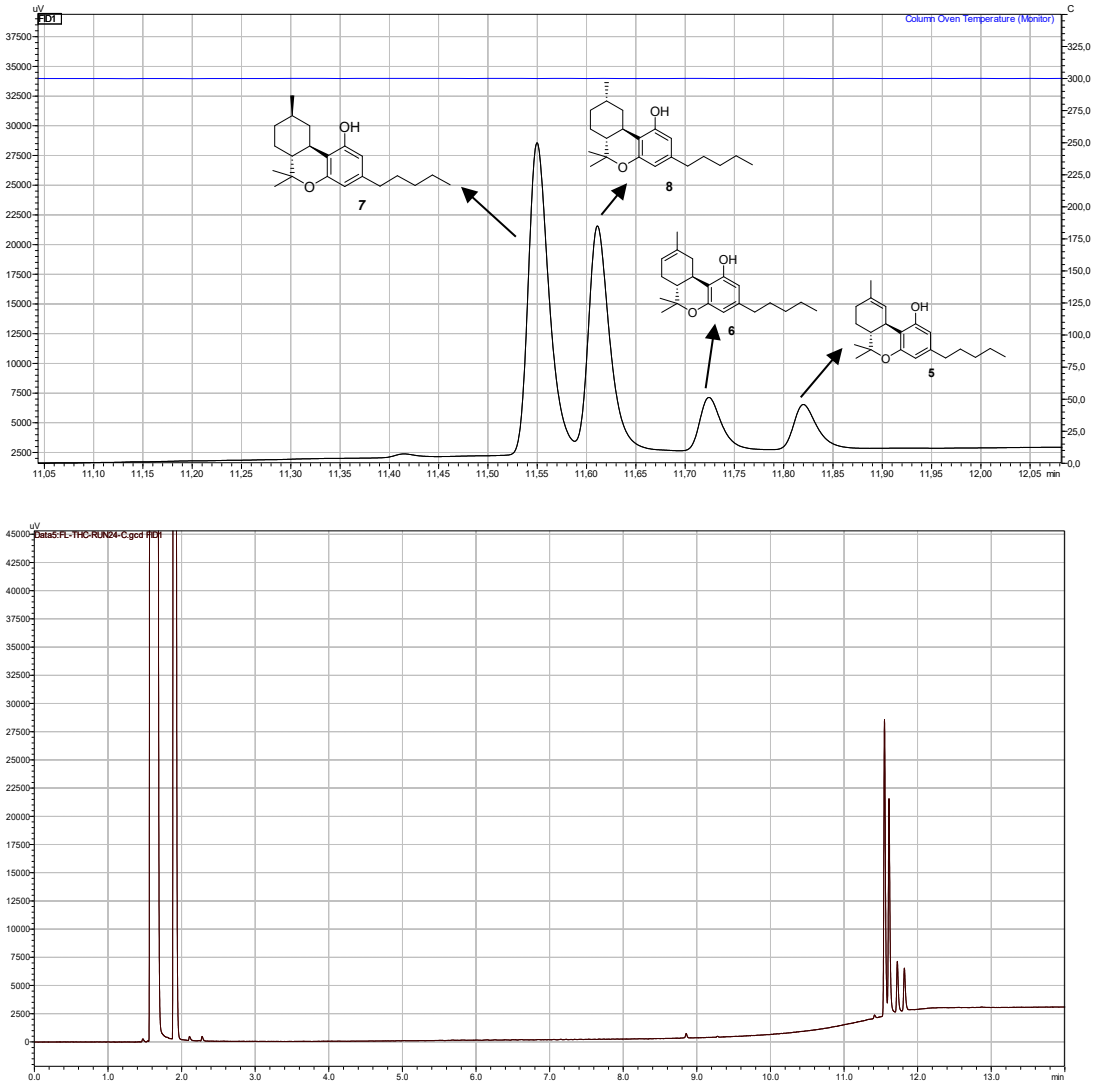

*Figure S 2: Example of GC-FID Chromatogram for the hydrogenation of Δ9-THC (**5**) to HHC over Pt/alumina. Retention times: R¬HHC (**7**) 11.55 min; S-HHC (**8**) 11.62 min; Δ^8-THC 11.72 min (**6**); Δ^9-THC 11.82 min (**5**). Top – Zoomed in chromatogram; Bottom – Full chromatogram.*

The results obtained with the GCFID were validated using ^{1}H-NMR. The parity plots are reported in Figure S 3.

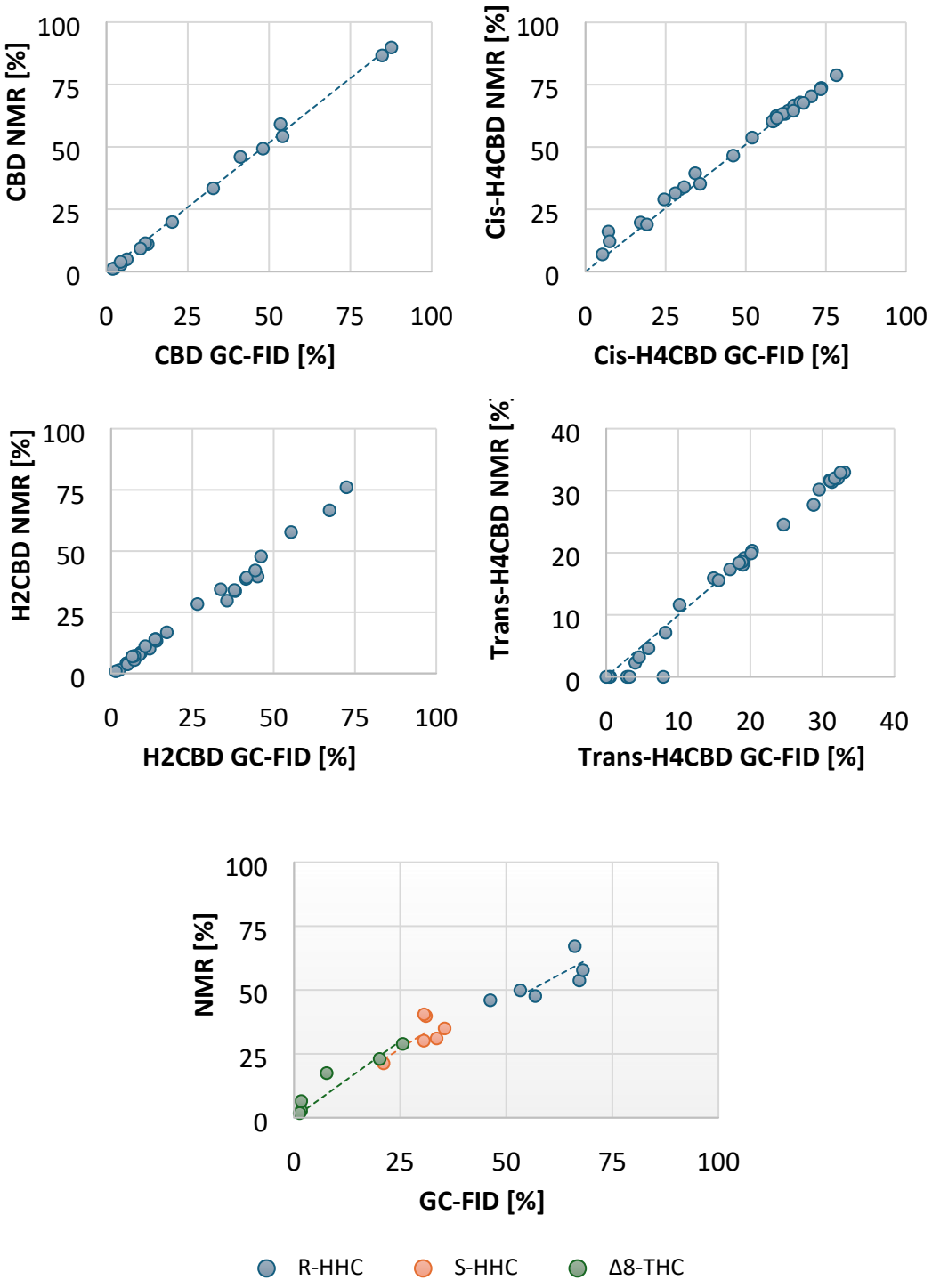

Figure S 3: Parity plots for the content of different species, as measured by NMR and GC-FID.

1.4. GC-MS Analysis

GC-MS analysis was performed using a Shimadzu GCMS-QP2010 SE, using an RTX5MS column (30 m x 0.25 mm x 0.25 µm) and helium as carrier gas with a linear velocity of 40 cm/sec. The injector temperature was set to 280 °C. After 1 min at 50 °C, the oven temperature increased by 25 °C/min to 300 °C and kept for 3 min. The mass detector

was a quadrupole with pre rods and electron impact ionization. The following settings were used in the detector: ion source temperature 200 °C, interface temperature 310 °C, solvent cut time 2.5 min, acquisition mode scan, mass range m/z = 50400. The spectra are reported at the end of this document from Figure S 31 to Figure S 37.

1.5. ICP-MS Analysis

The leaching of platinum was assessed by inductively coupled plasma mass spectrometry (ICPMS) (Agilent 7900). Three liquid samples were submitted, all from the processing of CBD. Before the ICP-MS analysis, the samples were diluted with ultrapure water and 1%$_v$ HNO_3 + 0.5%$_v$ HCl. All the samples showed negligible amounts of metal (<1 ppb).

1.6. SEM and EDS Images

Scanning electron microscopy (SEM) images and energy dispersive X-ray spectroscopy (EDS) analysis were performed using a Zeiss Gemini DSM 982 field emission SEM. The EDS-based quantitative elemental analysis and element distribution mapping were performed using an Oxford Instruments Ultim Max 40 silicon drift detector. All imaging and EDS analyses were made with an acceleration voltage of 10 kV and a working distance of 11 mm. For quantification and EDS map generation, we used the software package provided with the Oxford Instruments AZTec (v.6.1), using the available standard EDS quantification library. In the following section we report three SEM imaging with the EDS traces for Pd/alumina (Figure S 4, Table S 2), Pt/alumina (Figure S 5, Table S 3) and Ru/alumina (Figure S 6, Table S 4).

1.6.1. Pd/alumina

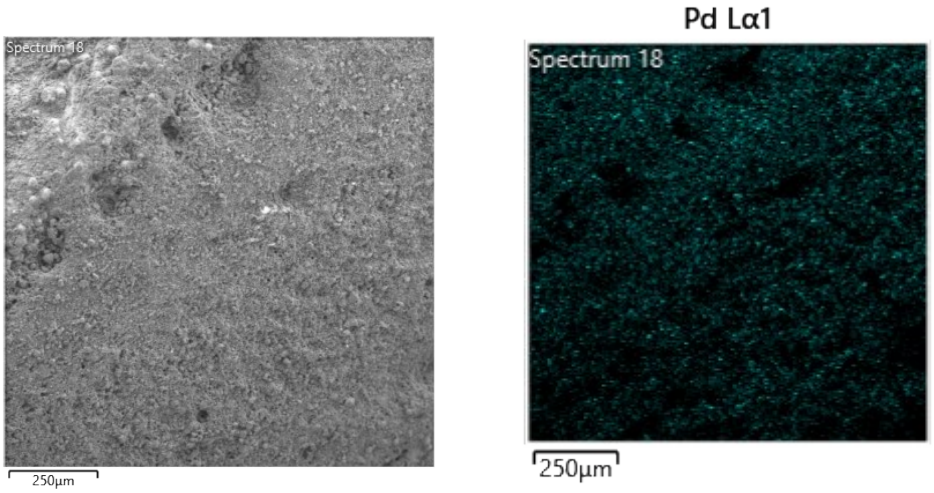

Figure S 4: SEM and EDS measurement for palladium on alumina CSM.

Table S 2: Elemental content for the CSM.

Element	Line	%w	Error %w
O	K series	42.06	
F	K series	1.03	0.06
Al	K series	44.39	0.16
S	K series	0.42	0.03
Cl	K series	0.59	0.04
Cr	L series	0.00	1.37
Fe	L series	1.61	0.20
Pd	L series	9.91	0.16
Total		100.00	

1.6.2. Pt/alumina

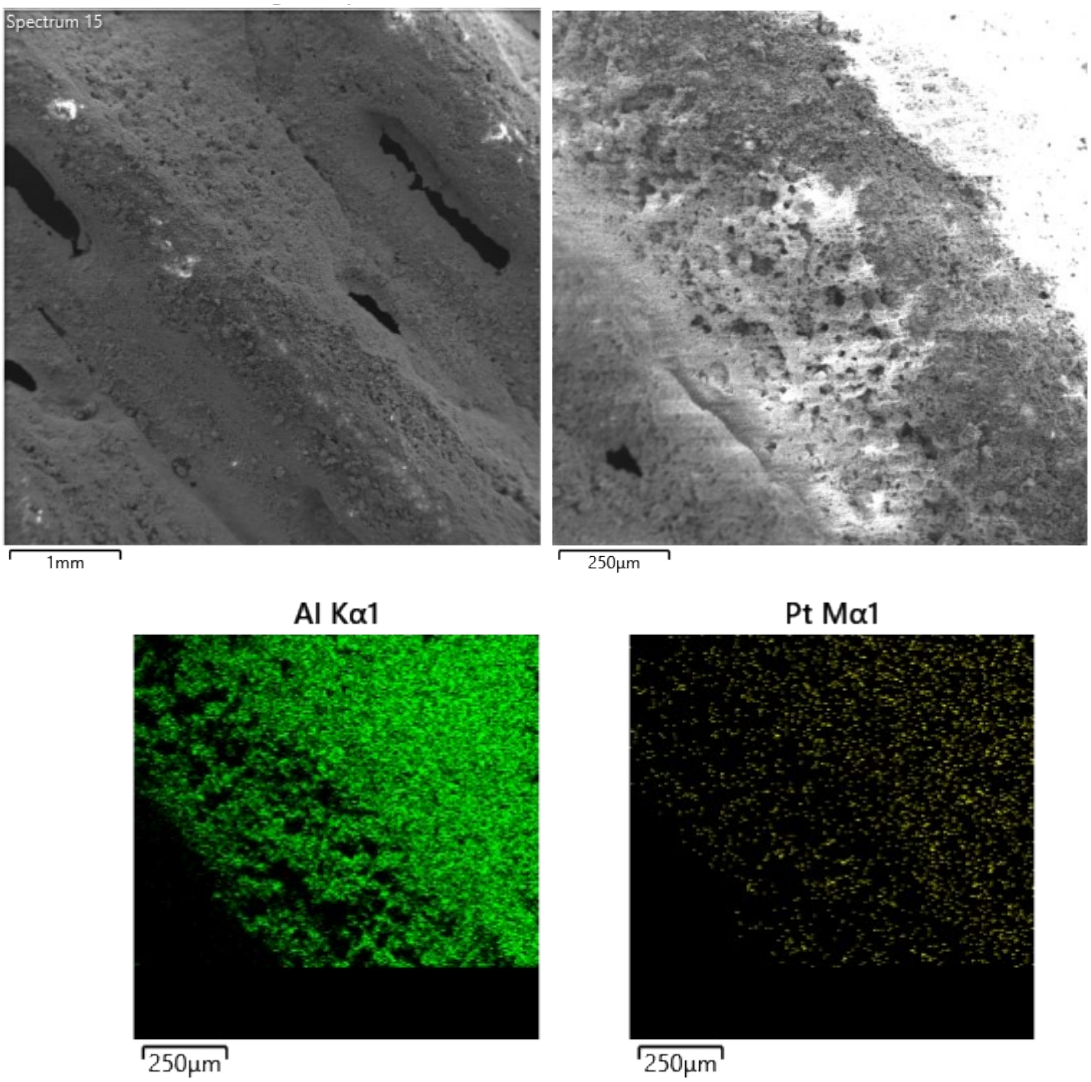

Figure S 5: SEM and EDS imaging of two sections of a platinum on alumina CSMs.

Table S 3: Elemental content for the CSM.

Element	Line	%w	Error %w
O	K series	42.13	0.20
F	K series	0.77	0.07
Na	K series	0.34	0.04
Al	K series	46.87	0.21
Si	K series	3.24	0.07
Ni	L series	1.22	0.12
Pd	L series	0.00	0.15
Pt	M series	5.44	0.26
Total		100.00	

1.6.3. Ru/alumina

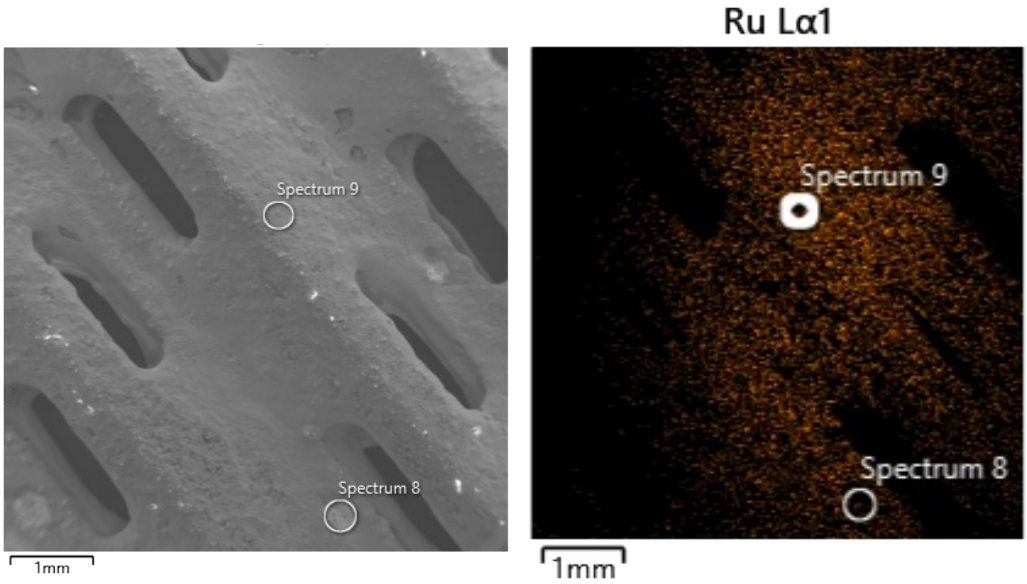

Figure S 6: SEM and EDS measurement for ruthenium on alumina CSM.

Table S 4: Elemental content for the CSM.

Element	Line	%w	Error %w
O	K series	46.49	0.17
Na	K series	0.33	0.04
Al	K series	47.48	0.17
P	K series	0.00	0.04
S	K series	0.17	0.04
Cl	K series	0.50	0.07
Fe	L series	0.00	0.23
Ru	L series	5.04	0.19
Total		100.00	

1.7. Experimental Setup

A labeled image of the flow configuration is given in Figure S 7. The liquid feed was delivered by a HPLC pump (Knauer AZURA P 4.1S). Hydrogen was delivered by a H-Genie hydrogen generator (ThalesNano), with an integrated mass flow controller (MFC), operated with HPLC grade water. The HGenie was also fitted with a pressure sensor to monitor the pressure of the whole setup. A sixway valve was used for screening experiments. Either a 4 mL or a 10 mL sample loop was used in the screening experiments. The gas and the liquid streams were combined in a Y-connector made of PEEK, immediately before entering the Ehrfeld Modular MicroReaction System (MMRS) system via a 1/16” input connector, through transparent tubing (PFA, 0.8 mm i.d.). The hydrogenation reactions were performed using an Ehrfeld Miprowa reactor (0224-2-

2004-F, Hastelloy C-276). This reactor comprises 8 channels with a rectangular cross-section (1.5 mm x 12 mm x 300 mm), and an internal volume of each channel, after the insertion of the CSMs, previously estimated by Lebl to be 3.4 mL.[1] Only 4 channels were used during this investigation (i.e. half of the reactor). Each channel can house up to 2 CSMs. During the investigation, either 1 (limonene hydrogenation only), 2 or 4 CSMs were used, and they were housed in the top channels (i.e. 5A, 5B, 8A and 8B, where A and B refer respectively to the right and the lefthand side of the channel). The remaining channels were filled with stainless steel fishbone mixers. The temperature of the reactor was controlled by a Huber CC-304 thermostat and was monitored by an internal thermocouple located in the recirculation loop. After the reactor, the process stream was cooled down in a 1 mL stainless steel coil (0.8 mm i.d.) which was submerged in a water bath at room temperature. The pressure inside the system was then controlled by a back pressure regulator (BPR) (Equilibar HC 276, maximum pressure 34 Bar; max temperature 300 °C). At ambient pressure, the excess hydrogen was separated by a custom-made gas-liquid separator. The liquid stream was then collected into a flask for subsequent offline analysis and processing. A description of the CSMs and a description of the Miprowa reactor can be found in previous works.[1,2]

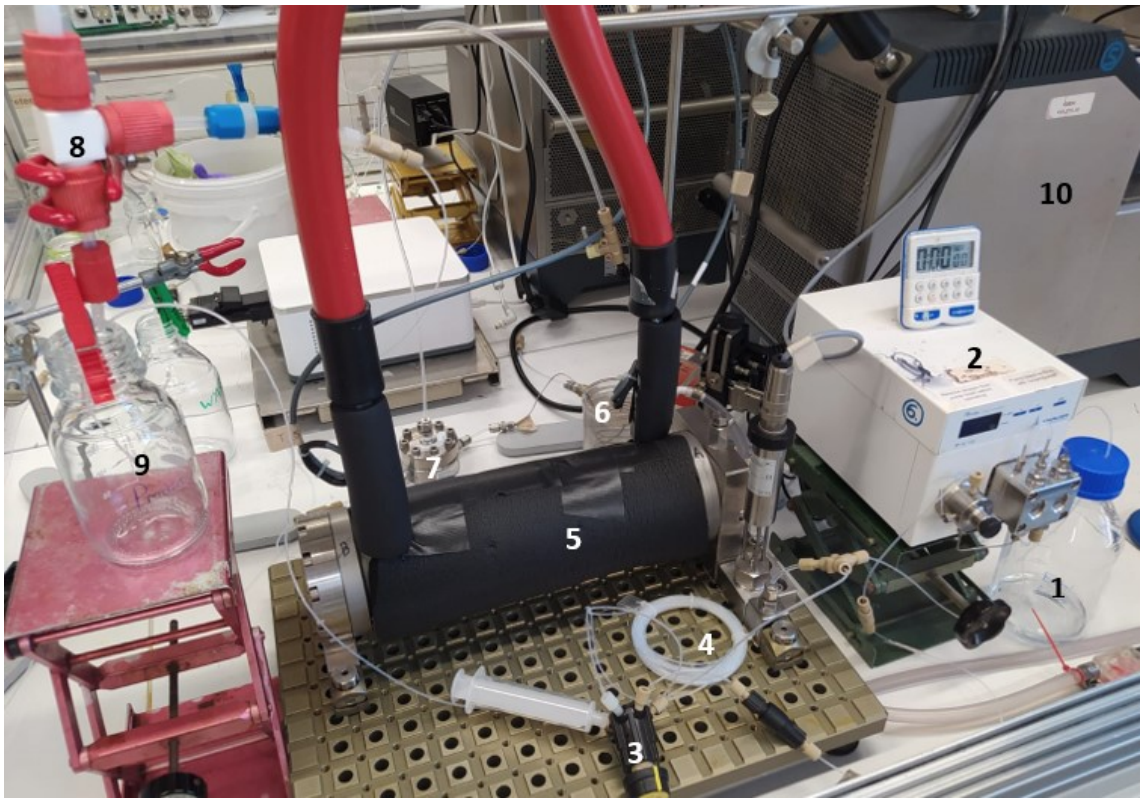

Figure S 7: Hydrogenation setup. Items: solvent reservoir (1), HPLC pump (2), six¬way valve (3), sample loop (4), Miprowa reactor (5), cooling coil (6), BPR (7), gas¬liquid separator (8), collection flask (9) and thermostat (10). The H¬Genie is not displayed.

1.8. Batch Synthesis of Δ^8-THC

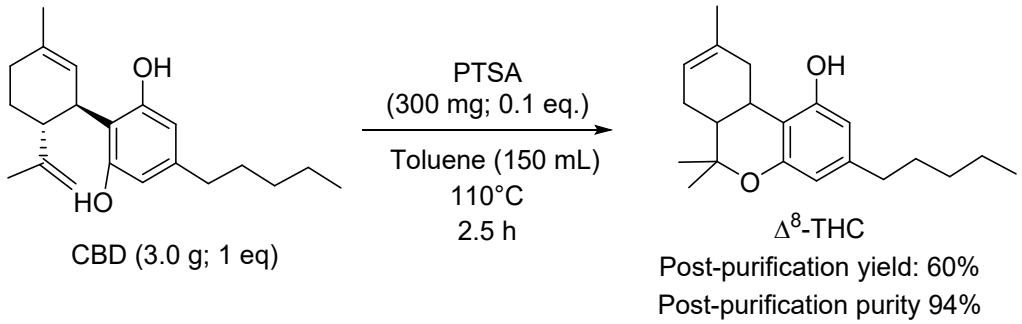

Scheme S 1: Reaction for the synthesis of Δ^8-THC.

A procedure described in literature was used.[3] The reaction is presented in Scheme S 1. CBD (3.0 g, 1 eq.) was inserted into a round flask along with a solution of *p*-toluene sulphonic acid (PTSA) (300 mg, 0.1 eq.) in toluene (150 mL) under a nitrogen atmosphere. The solution was refluxed at 110 °C for 2.5 h and then it was diluted with diethyl ether (200 mL) and poured into 100 mL of cold water. The upper layer was recovered, washed first with a saturated solution of $NaHCO_3$ (100 mL) and then with water (100 mL). The organic layer was then dried over Na_2SO_4 anhydrous, filtrated and

evaporated under vacuum. The recovered red oil was purified with column chromatography (Section 1.9) to obtain Δ^8-THC (1.93 g, yield 61%, purity 94%). The chromatogram of the compound post purification is represented in Figure S 8.

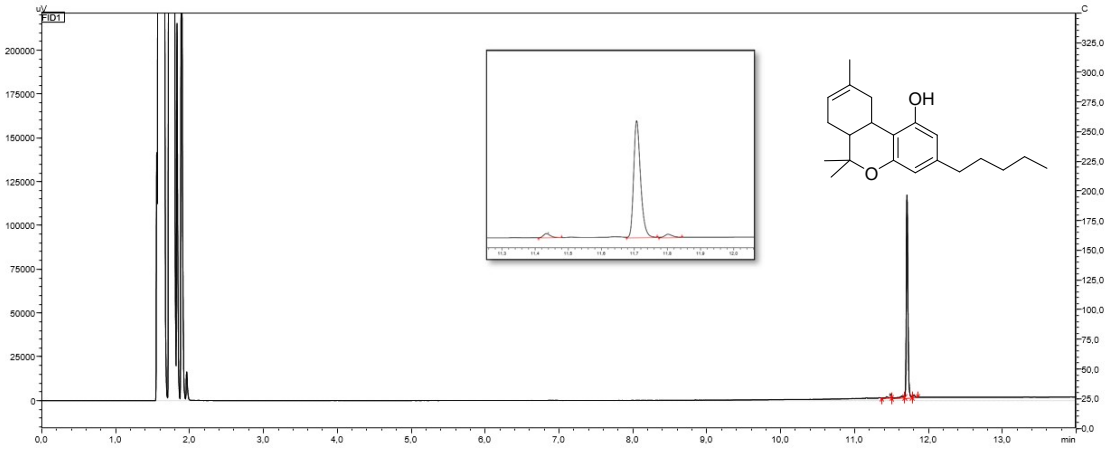

Figure S 8: GC-FID chromatogram of Δ^8-THC after purification. Some residual CBD and some Δ^9-THC can be observed in the smaller plot.

1.9. Purifications by Biotage Isolera

Purification of Δ^8-THC and H4CBD was performed using a Biotage Isolera 1. Ethyl acetate was used as high polarity solvent (A) and petroleum ether as low polarity solvent (B). Two wavelengths were set on the detector, 254 nm and 280 nm. Silica was used as a solid phase. Biotage DS 25 g columns were used. The gradients used for the purification of Δ^8THC and H4CBD are reported in Table S 5. Separation of H2CBD from CBD was attempted but proved to be challenging.

Table S 5: Gradients of solvents A used for the purification of Δ^8-THC and H4CBD.

Length	**Start**	**End**
[CV]	*[%]*	
3	0	0
10	0	3
15	3	5
5	5	10
10	10	10
7	10	25

2. Catalytic Static Mixer Results

2.1. Hydrogenation of CBD over Pd-electroplated (PdEP) CSMs

The results of the screening from the hydrogenation of CBD over Pd-electroplated CSMs are reported in the following sections.

2.1.1. Solvent Screening

The results for the experiments performed with either ethyl acetate or ethanol, at 60 °C and 100 °C, are reported in Table S 6. For all further experiments reported in the ESI, the solvent used was ethyl acetate.

Table S 6: Results for the solvent screening in the hydrogenation of CBD over Pd¬EP CSMs. Conditions: [0.09 M] CBD, 20 bar; H/S 11.3; 102 s.

Entry	Solvent	Temperature	Conversion	Selectivity			
			CBD	H2CBD	c-H4CBD	t-H4CBD	Imp.
		[°C]			*[%]*		
1	EtOH	60	14.3	81.9	0	3.1	15.0
2	EtOH	100	49.3	65.8	13.7	5.4	15.1
3	EtOAc	60	18.2	81.2	5.5	2.7	10.6
4	EtOAc	100	51.6	70.6	12.1	4.8	12.5

2.1.2. Temperature Screening

The results for the impact of temperature on the hydrogenation of CBD are reported in Table S 7.

Table S 7: Results for the temperature screening in the hydrogenation of CBD over Pd-EP CSMs. Conditions: [0.09 M] CBD, 20 bar; H/S 11.3; 102 s.

Entry	Temperature	Conversion	Selectivity			
		CBD	H2CBD	c-H4CBD	t-H4CBD	Imp.
	[°C]			*[%]*		
1	60	18.2	81.2	5.5	2.7	10.6
2	100	51.6	70.6	12.1	4.8	12.5
3	120	83.2	47.7	27.3	11.6	13.5
4	140	89.7	36.1	35.5	15.7	12.7

2.1.3. Residence Time Screening

The results for the screening of different residence times for the hydrogenation of CBD at 140 °C are reported in Table S 8. There was evidence of deactivation due to the irregularity in the trend with increasing residence time at the same temperature.

Table S 8: Results for the screening of residence time in the hydrogenation of CBD over Pd-EP CSMs. Conditions: [0.09 M] CBD, 20 bar; H/S 11.3; 140 °C.

Entry	Residence Time	Conversion	Selectivity			
		CBD	H2CBD	c-H4CBD	t-H4CBD	Imp.
	[s]			*[%]*		
1	102	89.7	36.1	35.5	15.7	12.7
2	204	89.3	42.1	30.0	15.7	12.2
3	408	91.6	42.5	27.4	17.2	12.8

2.2. Hydrogenation of CBD over Pd/alumina CSMs

The results of the screening for the hydrogenation of CBD over Pd/alumina CSMs are reported in the following sections.

2.2.1. H/S Ratio Screening

The hydrogen to substrate ratio (H/S) was screened at 25 mL_n/min and 75 mL_n/min, at 140 °C and at a liquid flow of 2 mL/min. The results are presented in Table S 9.

Table S 9: Results for the H/S ratio screening in the hydrogenation of CBD over Pd/alumina CSMs. Conditions: [0.1 M] CBD, 20 bar, 102 s, 140 °C.

Entry	H/S Ratio	Conversion	Selectivity			
		CBD	H2CBD	c-H4CBD	t-H4CBD	Imp.
	[-]			*[%]*		
1	5.7	98.9	7.6	48.1	25.8	18.5
2	17.2	98.9	7.3	48.3	26.5	17.9

2.2.2. Temperature Screening

The results for the screening of the hydrogenation of CBD at different temperatures in the range 60 to 160 °C are reported in Table S 10.

Table S 10: Results for the temperature screening in the hydrogenation of CBD over Pd/alumina CSMs. Conditions: [0.1 M] CBD, 20 bar; H/S 11.3, 102 s.

Entry	Temperature	Conversion	Selectivity			
		CBD	H2CBD	c-H4CBD	t-H4CBD	Imp.
	[°C]			*[%]*		
1	60	64.5	44.3	21.8	9.8	24.1
2	100	95	14.9	46.9	21.6	16.6
3	120	98	7.5	54.4	25.2	12.9
4	140	99.2	4.1	58.7	27	10.2
5	160	99.7	3.0	58.5	28.5	10.1

2.2.3. Long Run with CBD at 160 °C

The system was operated for a total of 40 min. During the experiment, 8 fractions were collected and analyzed by GCFID. The results are presented in Table S 11 and Figure S 9.

Table S 11: Long run with Pd/alumina CSMs. Conditions: [0.1 M] CBD, 160 °C, 20 bar, 102 s, H/S 11.3.

Sample	Collection Time	Conversion	Selectivity				Cis:Trans
		CBD	H2CBD	c-H4CBD	t-H4CBD	Imp.	
	[min]			*[%]*			*[-]*
1	5	99.6	3.6	54.9	28.6	12.9	1.92
2	10	99.7	4.1	54.2	28.9	12.7	1.88
3	15	99.7	4.4	53.3	28.6	13.7	1.86
4	20	99.6	4.9	53.2	27.8	14.0	1.91
5	25	99.6	4.9	51.2	28.5	15.4	1.80
6	30	99.2	5.9	50.1	26.8	17.1	1.87
7	35	99.4	5.7	50.0	27.0	17.2	1.86
8	40	99.5	5.9	49.3	26.8	17.8	1.84
Average		99.5	4.9	52.0	27.9	15.1	1.87

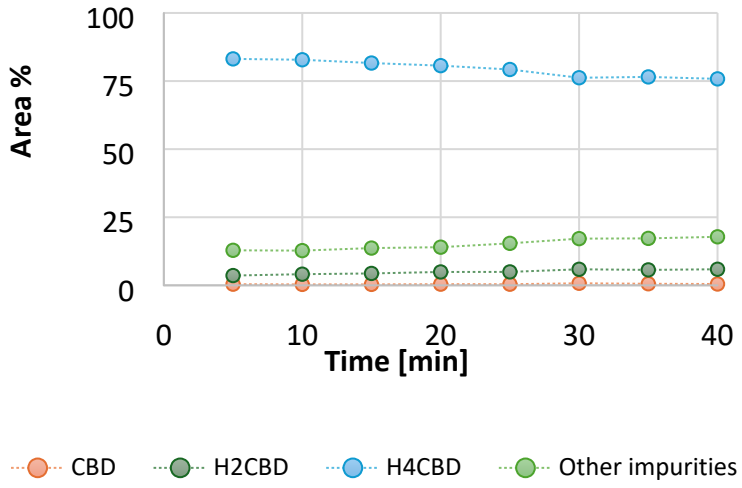

*Figure S 9: Long run trend for the reaction of CBD (**1**) at 160 °C, see Table S11 for the full set of conditions.*

2.3. Hydrogenation of THC over Ru/alumina CSMs

2.3.1. Temperature Screening

The results from the screening of temperature for the hydrogenation of Δ^8-THC over Ru/alumina CSMs are reported in Table S 12 and Figure S 10. No impurities were observed.

Table S 12: Results for the temperature screening in the hydrogenation of Δ^8-THC over Ru/alumina CSMs. Note: different Conditions: [0.1 M] Δ^8-THC, 20 Bar, 408 s, H/S 178.

Entry	Temperature	Conversion	Selectivity	
		Δ^8THC	RHHC	SHHC
	[°C]		*[%]*	
1	70	74.3	54.2	45.8

2	80	76.1	56.2	43.8

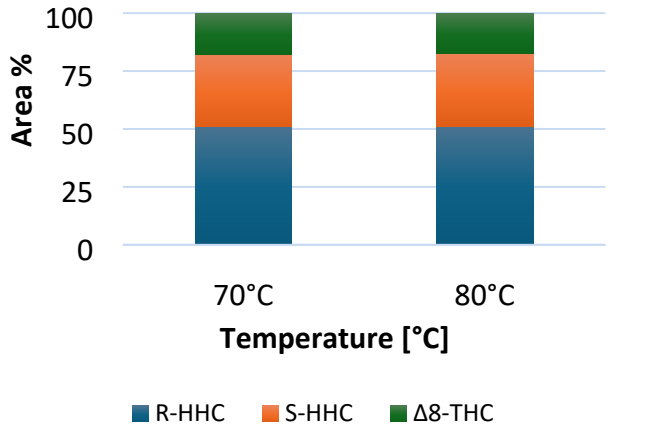

Figure S 10: Results for the temperature screening as area %.

2.3.2. Catalyst Recoverability by Washing with Acetone

The influence of an acetone wash on the recoverability of the catalyst was investigated by testing the hydrogenation of CBD over a previously used Ru/alumina CSM at 60 °C, 102 s and 20 Bar. The catalyst was first washed online with pure ethyl acetate during a long run where the performance was decreasing over time (Figure S 11). After washing, no changes were seen regarding the performance of the catalyst. The catalyst was then tested at 60 °C, taken offline, washed with acetone and re-tested and the results are reported in Figure S 12. A strong recovery in activity was observed as demonstrated with the increase in H4CBD formed.

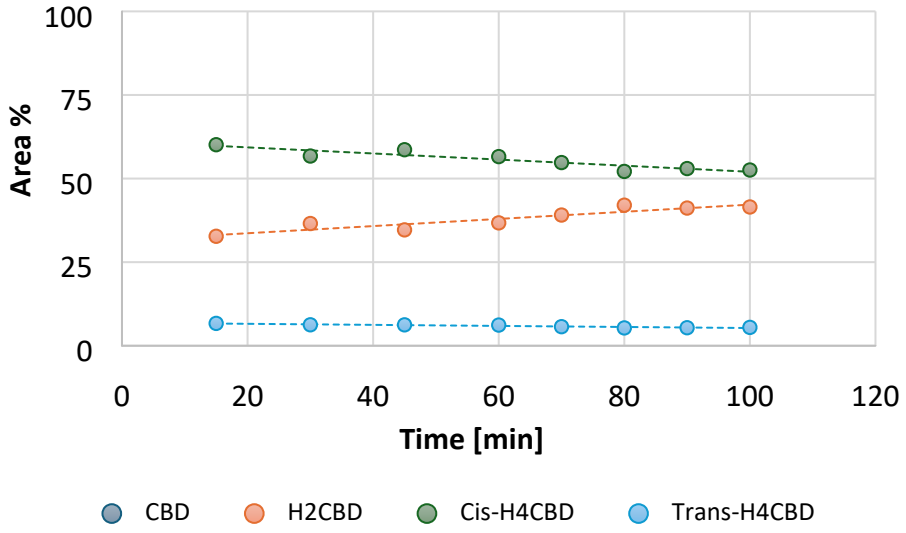

Figure S 11: Long run for the conversion of CBD over Ru/alumina with a washing step at 45 min.

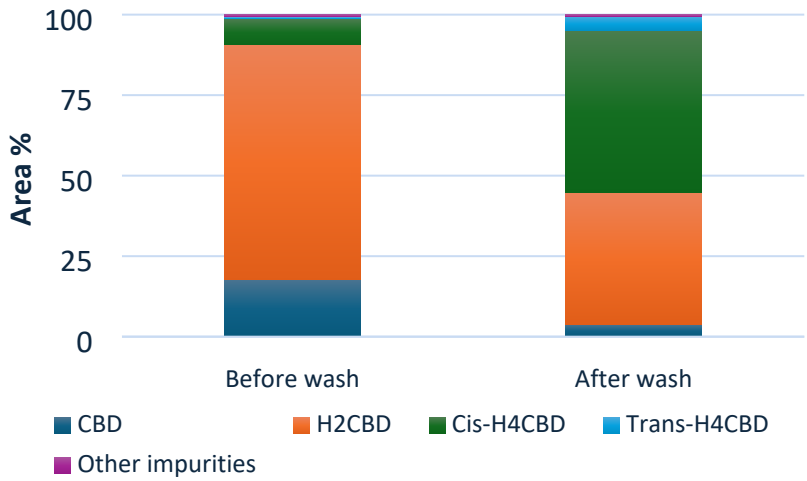

Figure S 12: Results for the conversion of CBD over Ru/alumina before and after a washing step with acetone. The increase in H4CBD after a wash demonstrated the increase in the catalytic activity.

2.4. Hydrogenation of CBD over Pt/alumina CSMs

The results of the screening for the hydrogenation of CBD, H2CBD and THC over Pt/alumina CSMs are reported in the following sections.

2.4.1. Blank Experiment

The Blank experiments were performed with a 0.1 M solution of CBD at 60 °C and 80 °C, 408 s, 20 bar, over Pt/alumina CSMs, without hydrogen. The GC profiles before and after the run are reported in Figure S 13. No conversion of CBD or formation of impurities were observed.

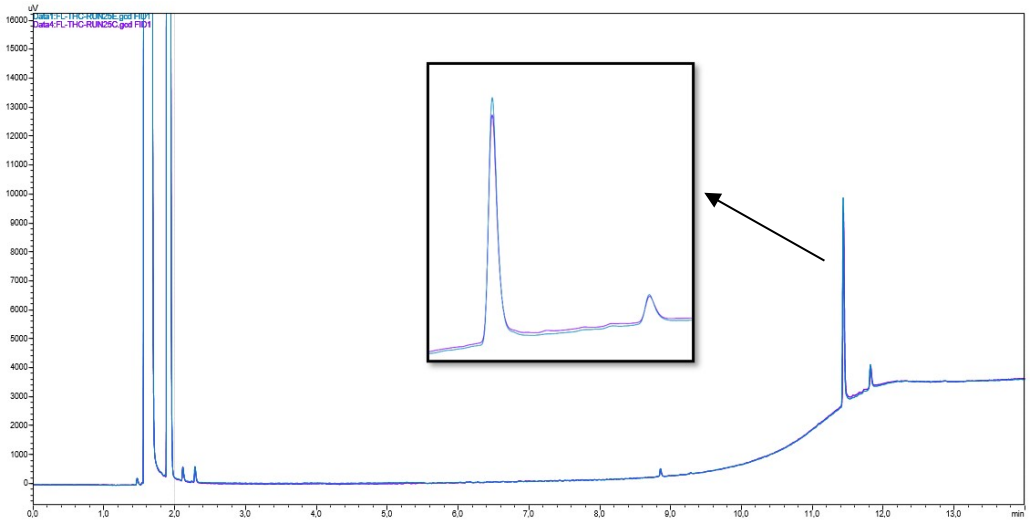

Figure S 13: GC-FID traces of the blank experiment (CBD peak in the square).

2.4.2. H/S Ratio Screening

The results from the screening of the hydrogen flow rates to avoid mass transfer limitations are reported for two residence times in Table S 13 and in Figure S 14.

Table S 13: Results for the screening of different hydrogen flows at different residence times. Conditions: [0.1 M] CBD, 20 bar, 80 °C.

Entry	Residence Time	H2 Flow	Conversion	Selectivity			
			CBD	H2CBD	c-H4CBD	t-H4CBD	Imp.
	[s]	*[mL_n/min]*			*[%]*		
1	408	50	96.0	64.1	22.3	8.1	5.5
2	408	100	96.5	59.7	24.6	9.4	6.3
3	408	200	97.5	56.7	26.2	10.2	6.9
4	544	100	98.0	53.5	29.0	10.9	6.5
5	544	200	98.7	48.3	32.2	12.2	7.3
6	544	300	98.7	47.5	32.5	12.5	7.5

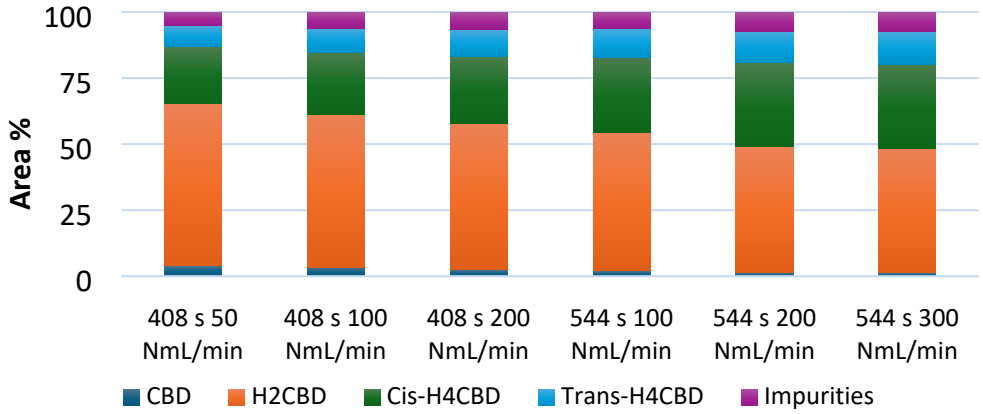

Figure S 14: Results for the screening of different hydrogen flow rates at different residence times.

2.4.3. CBD Concentration Screening

The results for the screening of different concentrations of CBD are reported in Table S 14 and in Figure S 15.

Table S 14: Results for the screening of concentrations. Conditions: [0.1 M] CBD, 20 bar, 65 °C, H/S 59.5.

Entry	Concentration	Residence Time	Conversion	Selectivity			
			CBD	H2CBD	c-H4CBD	t-H4CBD	Imp.
	[M]	*[s]*			*[%]*		
1	0.1	68	87.6	71.1	25.4	2.7	0.8
2	0.3	68	85.9	73.4	23.0	2.9	0.7
3	0.1	136	95.7	59.1	36.1	4.2	0.6
4	0.3	136	94.9	61.2	33.6	4.6	0.6

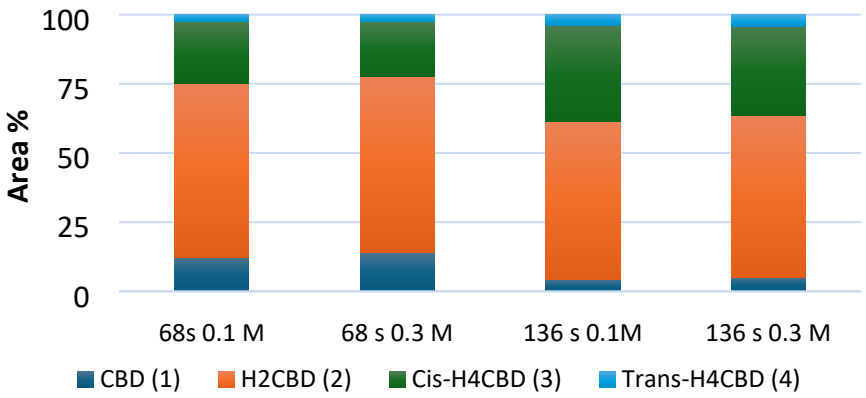

Figure S 15: Results for the screening of two different concentrations.

Further screening was performed with a concentration of CBD of up to 0.5 M, with the results shown in Table S 15 and Figure S 16. Some differences can be seen above 0.3 M, where the performance decreases. It is difficult to say if it is due to a change in kinetics or due to a faster rate of deactivation caused by an increase in concentration.

Table S 15: Screening of different concentrations of CBD. Conditions: 60 °C, 11 bar, 215 s, H/S 22.3.

Entry	Concentration	Conversion	Selectivity			
		CBD	H2CBD	c-H4CBD	t-H4CBD	Imp.
	[M]			*[%]*		
1	0.1	98.7	69.9	26.0	3.3	0.8
2	0.3	97.8	71.8	24.2	3.2	0.8
3	0.5	96.5	78.0	18.7	2.5	0.8

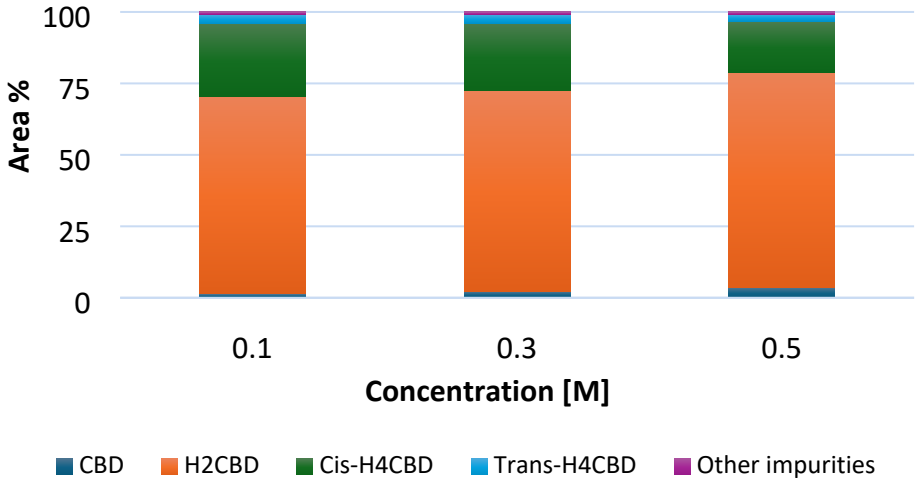

Figure S 16: Screening of different concentrations of CBD.

2.4.4. Design of Experiments (DoE): Influence of Temperature and Pressure

The factors and the levels used in the DoE are reported in Table S 16. The results of the DoE are reported in Table S 17.

Table S 16: Factors and Levels used for the DoE.

		-1	0	+1
Temperature	*[°C]*	60	80	100
Pressure	*[Bar]*	5.5	13	21

Table S 17: Results of DoE. Conditions: [0.1 M] CBD, 204 s; H/S 22.3.

Entry	**Temperature**	**Pressure**	**Conversion**	**Selectivity**			
			CBD	**H2CBD**	**c-H4CBD**	**t-H4CBD**	**Imp.**
	[°C]	*[bar]*			*[%]*		
1	100	21	>99	3.0	82.5	14.5	0
2	100	5.5	>99	1.2	81.6	17.2	0.1
3	80	13	>99	22.3	66.5	10.6	0.6
4	80	13	>99	25.8	63.4	10.2	0.6
5	60	21	98.2	76.6	20.8	2.2	0.4
6	60	5.5	99.1	67.4	27.7	3.8	1.1

The parity plots and the summary of fit obtained with Modde v.13 are reported in Figure S 17.

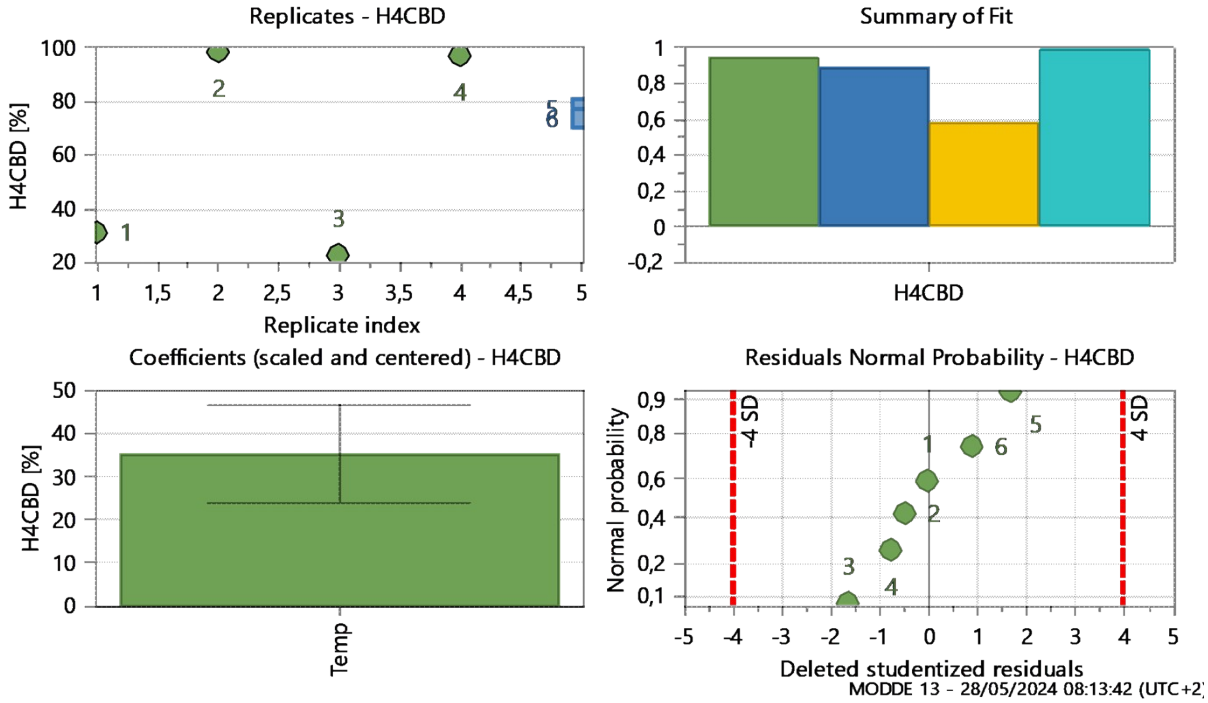

Figure S 17: Results from the analysis of the data in Modde.

2.4.5. Temperature Screening

The results for the screening in the range 60 to 100 °C are reported in Table S 18.

Table S 18: Results for the temperature screening over Pt/alumina. Conditions: [0.1 M], 20 bar, 102 s, H/S 11.2.

Entry	Temperature	Conversion	Selectivity			
		CBD	H2CBD	c-H4CBD	t-H4CBD	Imp.
	[°C]			*[%]*		
1	60	87.8	13.1	74.8	9.7	2.4
2	80	94.8	9.6	78.4	10.6	1.4
3	100	98.1	5.1	82.9	10.8	1.2

2.4.6. Residence Time Screening

The results for the screening in the range 204 to 544 s, at 80 °C are reported in Table S 19.

Table S 19: Results of the residence time screening over Pt/alumina CSMs. Conditions: [0.1 M] CBD, 80 °C, 20 bar. The H/S ratio varied based on the liquid flow rate at a fixed gas flow of 200 mL_n/min.

Entry	Residence Time	Conversion	Selectivity			
		CBD	H2CBD	c-H4CBD	t-H4CBD	Imp.
	[s]			*[%]*		
1	544	>99	1.0	80.0	18.5	0.5
2	408	>99	2.1	74.8	22.6	0.5
3	272	99.3	6.0	73.5	19.5	1.0
4	204	98.9	11.9	69.9	16.5	1.7

2.4.7. Long Run for the Hydrogenation of CBD to H4CBD Based on Unoptimized Conditions

The system was operated for 90 min with a 0.1 M feed solution of CBD. The solution was pumped at a flow rate of 1.50 mL/min, giving a residence time of 272 s. The reaction temperature was 80 °C. During the experiment 6 fractions were collected and analyzed on the GC-FID (Table S 20 and Figure S 18). The solvent was removed under vacuum to obtain 5.03 g of crude product mixture.

Table S 20: Measured conversion and selectivity during the long run for the preparation of H4CBD.

Entry	Collection Time	Conversion	Selectivity				Cis:Trans
		CBD	H2CBD	c-H4CBD	t-H4CBD	Imp.	
	[min]			*[%]*			*[-]*
1	15	99.4	12.0	70.2	16.0	1.8	4.4
2	30	99.3	13.3	69.6	15.2	1.9	4.6
3	45	99.3	12.5	70.2	15.5	1.8	4.5
4	60	99.4	12.1	71.4	14.7	1.9	4.9
5	75	99.4	12.2	71.6	14.3	1.9	5.0
6	90	99.4	13.6	69.4	15.0	2.0	4.6
Average		99.4	12.6	70.4	15.1	1.9	4.7

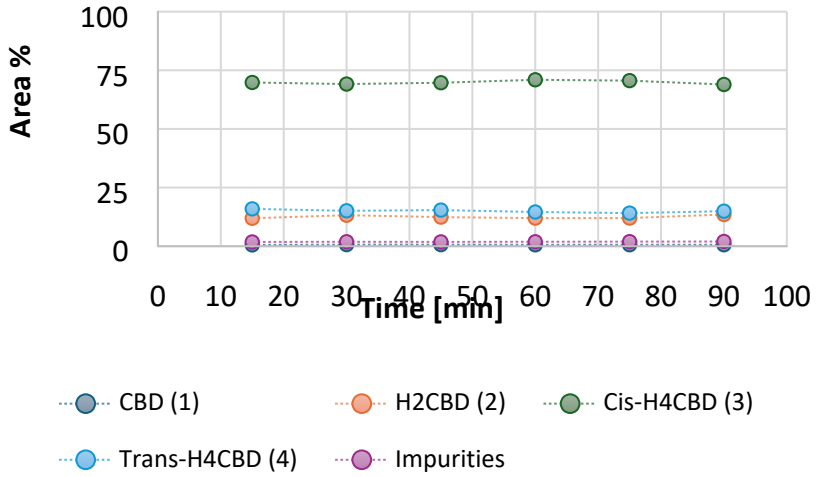

Figure S 18: Results in area % over time in the long run for the preparation of H4CBD

2.4.8. Long Run for the Synthesis of H4CBD at Optimized Conditions

The system was operated for 180 min with a 0.1 M solution of CBD at 80 °C. The solution was pumped at a flow rate of 0.75 mL/min, giving a residence time of 544 s. The H/S ratio was equal to 119. During the experiment, 6 fractions were collected and analyzed on the GC-FID (Table S 21). The solvent was removed under vacuum to afford H4CBD (3.69 g, 86% yield, 92.3% purity, cis:trans ratio 5.5) as a transparent oil. The productivity was about 1.23 g/h.

Table S 21: Results for the long run for the preparation of H4CBD

Sample	**Collection Time**	**Conversion**	**Selectivity**				**Cis:Trans**
		CBD	**H2CBD**	**c-H4CBD**	**t-H4CBD**	**Imp.**	
	[min]			*[%]*			*[-]*
1	30	99.8	4.2	77.6	16.3	1.0	4.8
2	60	99.8	3.6	78.3	16.3	0.9	4.8
3	90	99.8	4.2	77.8	16.1	1.0	4.8
4	120	99.8	3.6	78.1	16.4	1.0	4.8
5	150	99.8	3.5	78.0	16.5	1.0	4.7
6	180	99.8	3.2	78.7	16.4	0.9	4.8
Average		99.8	3.7	78.1	16.3	1.0	4.8

2.4.9. Long Run for the synthesis of H2CBD at Optimized Conditions

The system was operated for 55 min with a 0.1 M feed solution of CBD. The solution was pumped at a flow rate of 2.0 mL/min, giving a residence time of 204 s. A H/S ratio of 11.7, a pressure of 11.2 bar and a temperature of 60 °C were used. During the experiment 4 fractions were collected and analyzed on the GC-FID (Table S 22). The solvent was removed under vacuum to give H2CBD (2.80 g, 89% purity) as a transparent

oil. Further purification of the product with column chromatography proved difficult due to the similarity of the compounds present in the mixture (CBD and H4CBD).

Table S 22: Conversion and selectivity in the long run for the hydrogenation of CBD to H2CBD

Entry	Collection Time	Conversion	Selectivity			
		CBD	H2CBD	c-H4CBD	t-H4CBD	Imp.
	[min]			*[%]*		
1	15	97.2	91.6	7.4	0.7	0.3
2	30	96.7	91.9	6.9	0.8	0.3
3	45	96.1	93.0	6.4	0.4	0.2
4	55	95.8	94.1	4.9	0.8	0.2
Average		96.5	92.7	6.4	0.7	0.3

2.5. Hydrogenation of H2CBD to H4CBD over Pt/alumina CSMs

2.5.1. Temperature Screening

The results for the screening of the hydrogenation of H2CBD at different temperatures are reported in Table S 23.

Table S 23: Results for the temperature screening for the synthesis of H4CBD from H2CBD. Conditions: 102 s; H/S 11.2, 20 bar.

Entry	Temperature	Conversion	Selectivity			
		CBD	H2CBD	c-H4CBD	t-H4CBD	Imp.
	[°C]			*[%]*		
1	60	99.7	20.4	70.5	8.2	0.9
2	80	99.8	12.2	77.3	9.8	0.7
3	100	>99	7.2	81.5	10.7	0.6

2.6. Hydrogenation of THC over Pt/alumina CSMs

2.6.1. Hydrogenation of Δ^9-THC: Screening of Temperature and Residence Time

The results for the screening of temperatures and residence time for the hydrogenation of Δ^9-THC are reported in Table S 24.

Table S 24: Results for the screening of temperature and residence time in the hydrogenation of Δ^9-THC. Conditions: [0.1 M], 20 bar. Note: a constant flow of 200 mL_n/min of H_2 was used.

Entry	Temperature	Residence Time	Conversion	Selectivity			
			Δ^9THC	RHHC	SHHC	Δ^8THC	Imp.
	[°C]	*[s]*			*[%]*		
1	60	408	92.3	51.3	39.0	9.2	0.5
2	70	408	98.4	60.6	34.0	4.9	0.5
3	80	204	95.0	56.6	35.3	7.7	0.4
4	80	408	99.5	67.0	30.9	1.7	1.1
5	80	544	99.7	67.7	30.5	1.3	1.1
6	90	408	>99	61.2	36.9	1.4	0.5

2.6.2. *Long Run for the Synthesis of HHC from Δ⁹-THC at Optimized Conditions*

The system was operated for 25 min with a 0.1 M solution of Δ⁹THC. The solution was pumped over 4 CSMs at a flow rate of 1.0 mL/min, giving a residence time of 408 s. A H/S ratio of 118, 20 bar and 80 °C were used. During the experiment 5 fractions were collected and analyzed on the GC-FID (Table S 25 and Figure S 19). The solvent was removed under vacuum to afford HHC (0.69 g, 87% yield, 97.7% purity, R:S ratio 2.4) as a transparent oil. The productivity of the process was equal to 1.62 g/h.

Table S 25: Conversion and selectivity in the long run for the hydrogenation of Δ⁹-THC.

Entry	Collection Time	Conversion	Selectivity			R:S
		Δ⁹-THC	RHHC	SHHC	Imp.	
	[min]		*[%]*			*[-]*
1	5	>99	69.4	30.6	-	2.3
2	10	>99	70.7	29.3	-	2.4
3	15	>99	71.3	28.7	-	2.5
4	20	>99	70.9	29.1	-	2.4
5	25	>99	71.0	29.0	-	2.4
Average		>99	70.7	29.3	-	2.4
NMR Average		>99	65.7	27	2.3	2.4

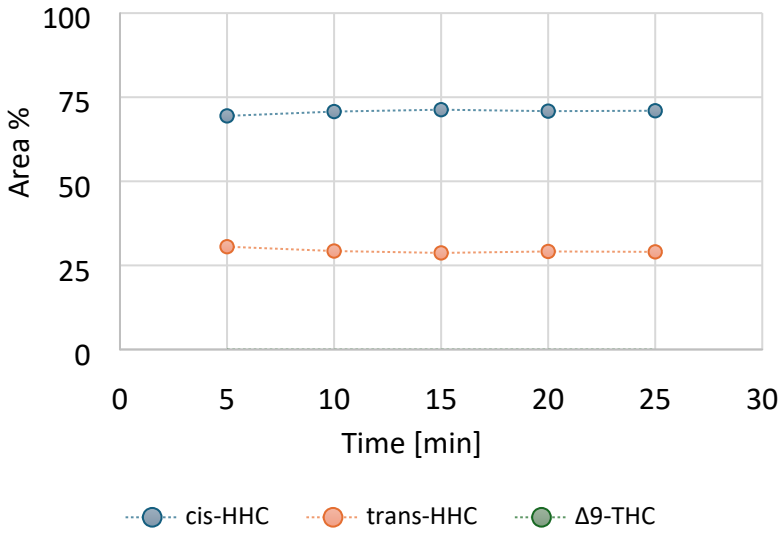

Figure S 19: Results in the long run for the hydrogenation of Δ⁹-THC.

2.6.3. *Hydrogenation of Δ⁸-THC: screening of Temperature and Residence Time*

The results for the screening of temperatures and residence time for the hydrogenation of Δ⁸-THC are reported in Table S 26. No impurities were observed.

Table S 26: Results for the screening of temperature in the hydrogenation of Δ⁸-THC. Conditions: [0.1 M], 408 s, 20 bar, H/S 89.

Entry	Temperature	Conversion	Selectivity	
		Δ⁸-THC	RHHC	SHHC
	[°C]		[%]	
1	60	90.7	56.7	43.3
2	70	95.1	64.0	36.0
3	80	98.3	68.4	31.6

2.6.4. Long Run for the Synthesis of HHC from Δ⁸-THC at Optimized Conditions

The system was operated for 55 min with a 0.1 M solution of Δ⁸-THC (94% purity of starting material). The solution was pumped at a flow rate of 1.0 mL/min, giving a residence time of 408 s. A H/S ratio of 118, 20 Bar and 80 °C were used. During the experiment 6 fractions were collected and analyzed on the GC-FID (Table S 27 and Figure S 20). The solvent was removed under vacuum to afford HHC (1.8 g, 97% yield, 94% purity) as a light brown oil. The throughput was equal to 1.8 g/h. The number of impurities remained constant at the same value as the starting solution. For this reason, the impurities are omitted in the table.

Table S 27: Conversion and selectivity in the long run for the hydrogenation of Δ⁸-THC.

Entry	Collection Time	Conversion	Selectivity		R:S
		Δ⁸-THC	RHHC	SHHC	
	[min]		[%]		[-]
1	5	99.2	64.4	35.6	1.8
2	15	98.7	63.7	36.3	1.8
3	25	98.5	62.9	37.1	1.7
4	35	98.4	62.6	37.4	1.7
5	45	97.9	62.2	37.8	1.6
6	55	97.9	62.2	37.8	1.6
Average		98.4	63.0	37.0	1.7

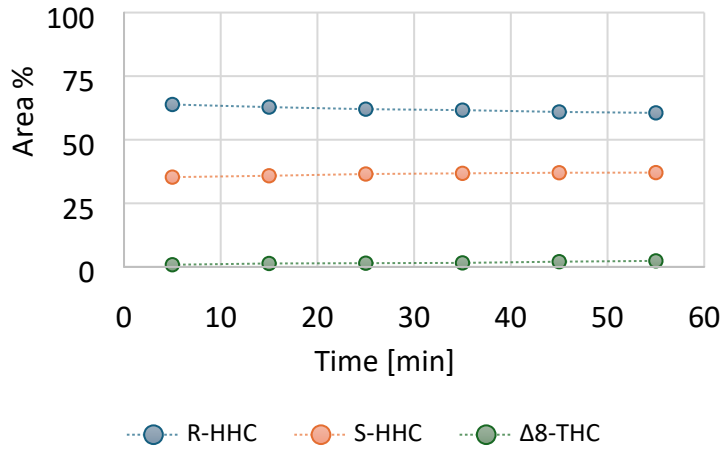

Figure S 20: Results for the long run for the hydrogenation of Δ⁸-THC.

3. Kinetics Investigation

3.1. Experimental Methods

3.1.1. Preparation of the Stock Solution

1 L of a [0.1 M] internal standard solution of hexadecane (22.645 g, 0.1 mol) was used to prepare a 1 L of a [0.1 M] solution of CBD (31.5 g, 0.1 mol).

3.1.2. Deconvolution of GCFID Peaks

Peak deconvolution was performed with hplcpy, a Python package developed by Chure and Cremer.[4] An example of a deconvoluted spectrum is reported in Figure S 21. The results obtained from the deconvolution of different mixtures were compared against those derived from a simple peak integration assuming peak splitting. The parity plot for this comparison is presented in Figure S 22. Overall, we observed that fitting the whole spectra did not yield good results as the size of the peaks of ISTD and compounds were quite dissimilar. We therefore decided to fit the two regions (ISTD and reaction peaks) separately. Moreover, the recognition of the small peaks was not always feasible (Figure S 21, left) and it was possible only for some of the spectra after changing of the input parameters. We therefore decided to use the simpler peak integration for kinetic analysis.

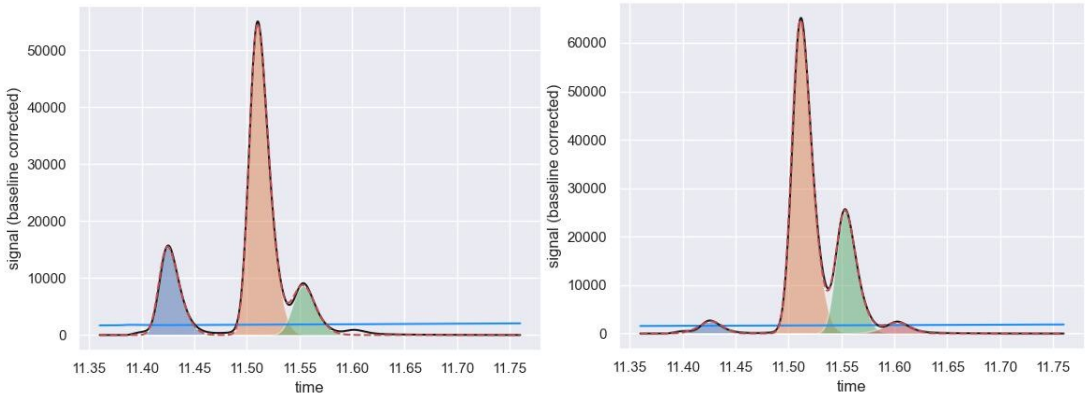

Figure S 21: Example of peak deconvolution. Left: small peak not detected. Right: Complete detection.

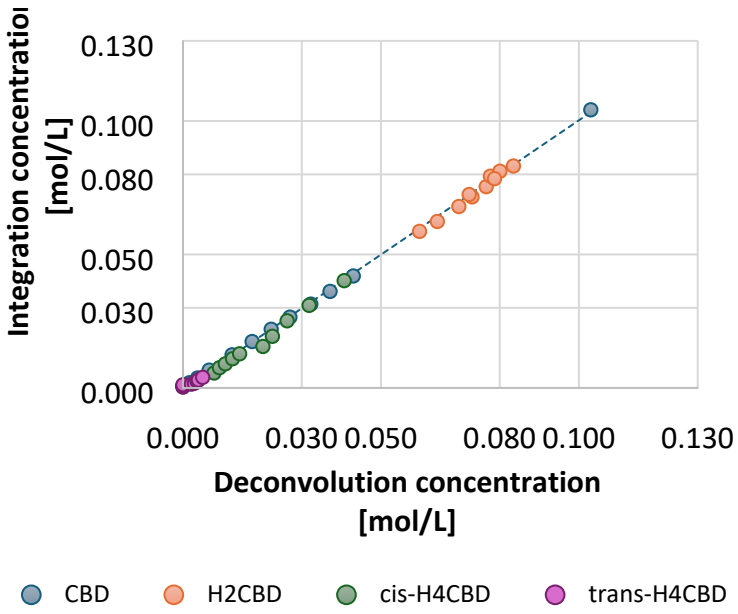

Figure S 22: Parity plot between the concentration measured by peak integration and that measured by peak deconvolution.

3.2. Kinetics Results

3.2.1. Matlab Model

Table S 28 reports the different sum of squares error (SSE) for the different scenarios considered in the kinetic fitting of the data measured at 60 °C.

Table S 28: Sum of square errors for different deactivation models, kd = rate constant for deactivation

	SSE
One kd for all	0.376
kd for H4CBD	0.417
kd for H2CBD	0.498
kd for cis-H4CBD	0.466
no kd	0.562

The fitted kinetic trends for Pt/alumina CSM (A) are reported in Figure S 23. The Arrhenius plot is presented in Figure S 24. The values of the kinetic constants are reported in Table S 29.

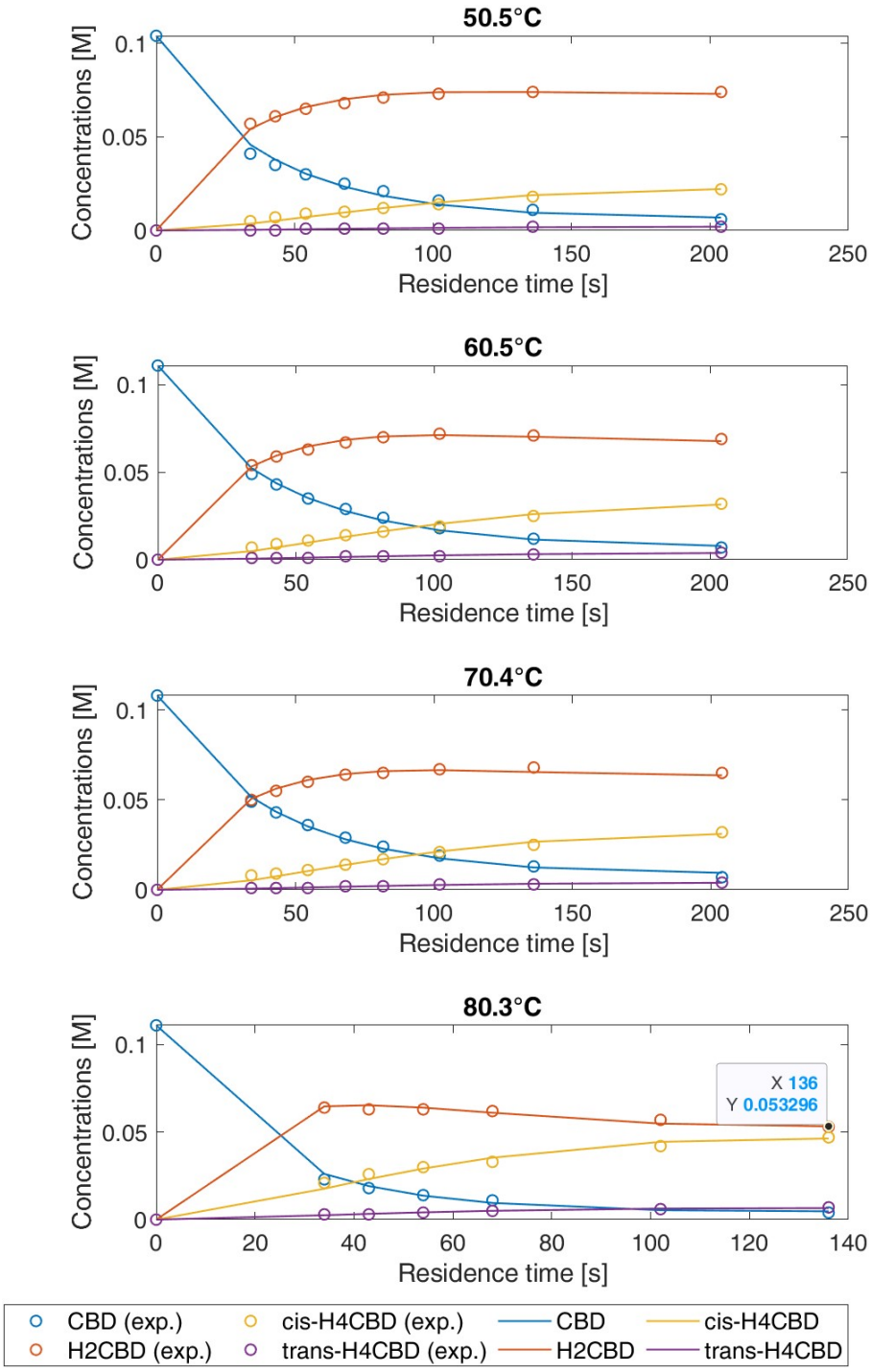

Figure S 23: Kinetic fittings at different temperature for CSMs A.

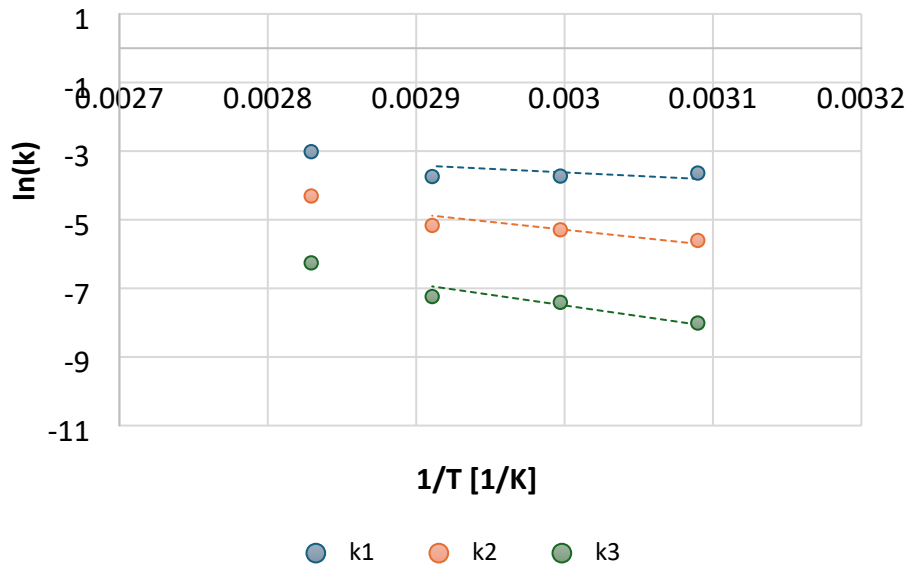

Figure S 24: Arrhenius plot for CSMs A.

Table S 29: Fitted kinetic constants for CSMs A at different temperatures.

Temperature	**k1**	**k2**	**k3**	**kd**
[°C]		*[1/s]*		
50.5	0.026	0.004	0.0003	0.0048
60.5	0.024	0.005	0.0006	0.0045
80.3	0.049	0.013	0.0019	0.0078
70.4	0.024	0.006	0.00072	0.0049

The errors of the Arrehenius parameters are reported in Table S 30.

Table S 30: Errors of Arrhenius fittings.

	k1		**k2**		**k3**		**kd**	
Fitting	-2078.8	2.615	-4581.7	8.454	-6224.8	11.18	-1669.1	-0.294
SE 95%	1614.9	4.777	1316.4	3.894	1297.5	3.838	1029.8	3.047
R2	0.453	0.314	0.858	0.256	0.920	0.252	0.568	0.200
F-test	1.657	2	12.11	2	23.02	2	2.627	2
SSreg. SSres.	0.163	0.197	0.791	0.131	1.46	0.127	0.105	0.0800

The fitted kinetic trends for Pt/alumina CSM (B) are reported in the manuscript. The Arrhenius plot is reported in Figure S 25.

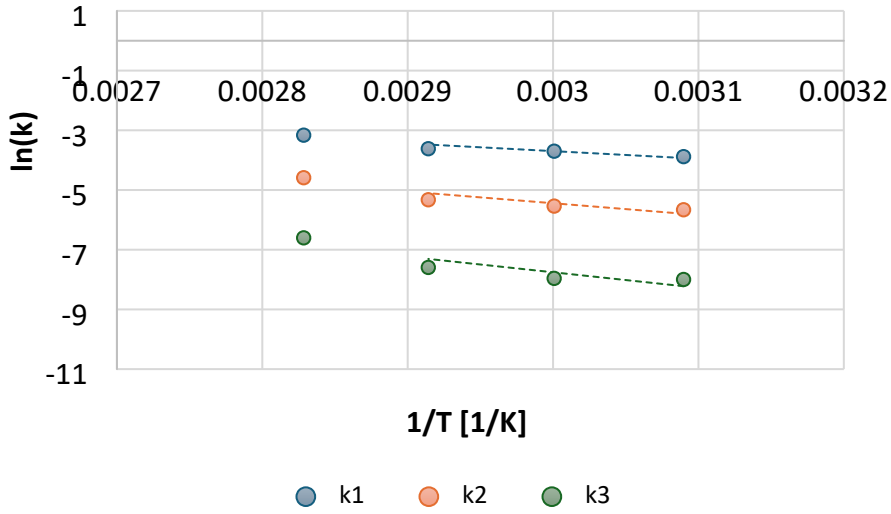

Figure S 25: Arrhenius plot for CSMs B.

The kinetic constants are in Table S 31.

Table S 31: Fitted kinetic constants for CSMs B at different temperatures.

Temperature	k1	k2	k3	deact
[°C]		*[1/s]*		
50.5	0.021	0.0035	0.00034	0.00237
60.1	0.025	0.0039	0.00035	0.00408
80.4	0.042	0.0102	0.00136	0.00500
70	0.027	0.0049	0.00050	0.00441

The errors of the Arrehenius parameters are reported in Table S 32.

Table S 32: Errors of Arrhenius fittings.

	k1		k2		k3		kd	
Fitting	-2569.2	4.010	-3930.3	6.348	-5207.4	7.866	-2666.0	2.320
SE 95%	633.6	1.875	1195.2	3.538	1779.8	5.268	845.5	2.503
R2	0.892	0.123	0.844	0.233	0.811	0.346	0.833	0.165
F-test	16.44	2	10.81	2	8.560	2	9.942	2
SSreg. SSres.	0.250	0.0304	0.585	0.108	1.027	0.2400	0.269	0.0542

3.2.2. Dynochem Model

The model structure fitted using the Dynochem software is reported at the top of Figure S 26. *Rxn4* is the deactivation of platinum. The middle section shows the general process scheme applied to the modeling and the bottom part the experimental scenarios that were fitted.

Reactions in Solution

Id	Reactants	→	Products	Bal	[+/-]
rxn1	CBD + H2 + Pt	→	H2CBD + Pt	✔	✔
rxn2	H2CBD + H2 + Pt	→	cis-H4CBD + Pt	✔	✔
rxn3	H2CBD + H2 + Pt	→	trans-H4CBD + Pt	✔	✔
rxn4	Pt	→	Pt_deact	✔	✔

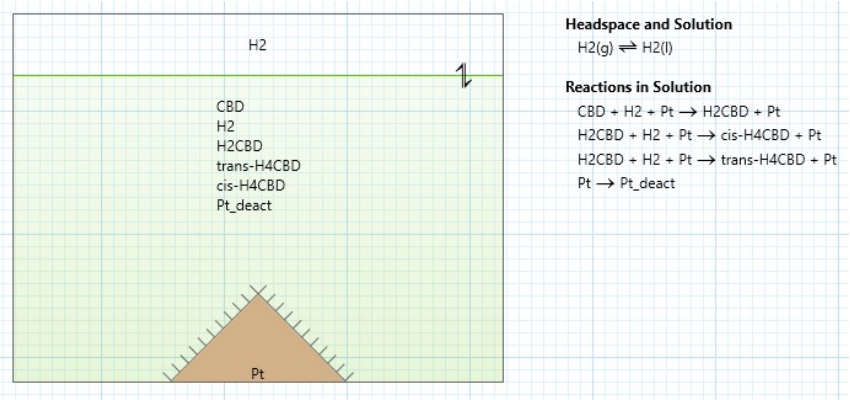

Scenarios

Model | Mass | Mole | Concentration | Equivalents

Id	Scenario	Solution Volume L	Solution Temperature C	Solution CBD mol/L	Solution Pt mol/L	Headspace Pressure bar	Headspace H2 mmol	Headspace kLac 1/s	GLE H2.Henry -
expt1	* Base Case 50.5°C	1	50.5	0.104176	0.0549	20	1000	0.5	9.46402
expt2	Base Case 80.4°C	1	**80.3**	**0.110988**	0.0549	20	1000	0.5	**7.45048**
expt3	Base Case 60.1°C	1	**60.5**	**0.11113**	0.0549	20	1000	0.5	**8.76411**
expt4	Base Case 70°C	1	**70.4**	**0.108275**	0.0549	20	1000	0.5	**8.095**

Figure S 26: Dynochem model.

3.2.3. Residence time vs. Real Residence Time

As mentioned in the manuscript, along one kinetic profile, the catalyst was operated for a given time which increases with residence time. This is because the points collected at longer residence times were also collected after the catalyst had been subjected to the flow of starting material for a time which equaled the sum of the purging time for all the points located ahead of a given point. This can be seen in Figure S 27. This implies that the rate of deactivation is distributed over a longer time than that assigned to the residence time.

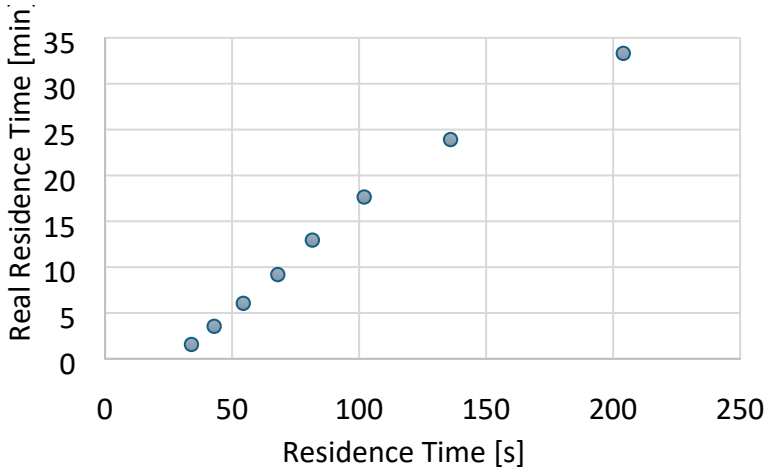

Figure S 27: Residence time vs. real residence time.

4. CSMs Deactivation Study

4.1. Experimental Methods

4.1.1. Reactor Configuration

Scheme S 2 pictures a schematic representation of the setup used in the study of the mechanism of deactivation using the hydrogenation of limonene to p-menthene and p-menthane (cis and trans), at different contents of resorcinol, as surrogate reaction.

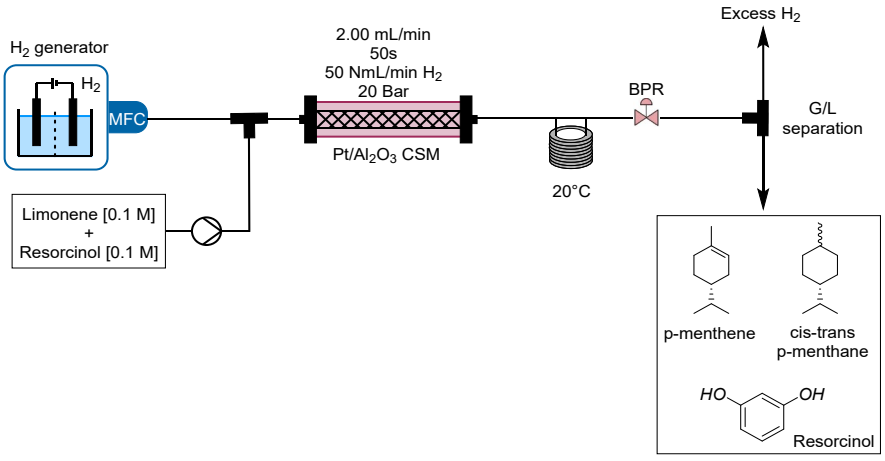

Scheme S 2: Experimental setup used for the hydrogenation of limonene.

4.1.2. GC-FID Chromatograms

A chromatogram of the different species forming from the hydrogenation is reported in Figure S 28. The chromatogram for a starting solution containing both limonene and resorcinol is reported in Figure S 29.

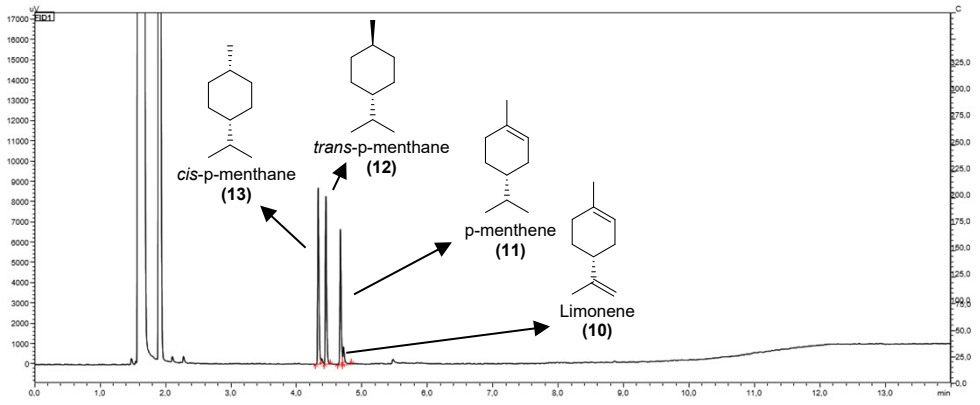

*Figure S 28: Example of GC-FID chromatogram for the product mixture derived from the hydrogenation of limonene. Retention times: Limonene (**10**) (4.72 min); p-menthene (**11**) (4.67 min); trans-p-menthane (**12**) (4.45 min); cis-p-menthane (**13**) (4.33 min).*

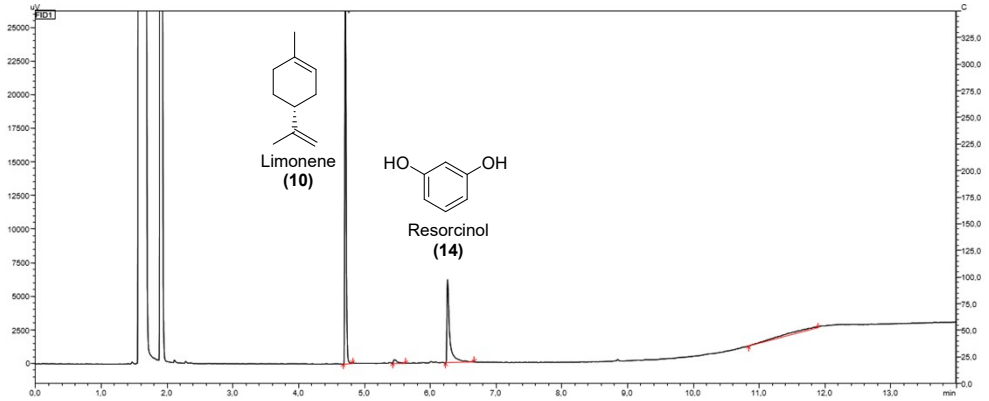

*Figure S 29: Example of GC-FID chromatogram of a mixture of limonene and resorcinol. Retention times: Limonene (**10**) (4.72 min); Resorcinol (**14**) (6.25 min).*

4.1.3. GC-FID Calibration for CBD

The calibration of CBD was performed at the concentrations reported in Table S 33, along with the ratios for the application of the internal standard calibration. The calibration plot is reported in Figure S 30.

Table S 33: GC-FID internal standard calibration.

Sample	**Concentration**		**C_{CBD}/C_{ISTD}**	**Area**		**A_{CBD}/A_{ISTD}**
	CBD	**ISTD**		**CBD**	**ISTD**	
	[M]		*[-]*	*[a.u.]*		*[-]*
0	0.297	0.099	2.985	143878	40148	3.584
1	0.223	0.099	2.238	98727	42658	2.314
2	0.148	0.099	1.492	68783	43328	1.588
3	0.074	0.099	0.746	31181	44971	0.693
4	0.028	0.099	0.280	12012	40148	0.299
5	0.0148	0.099	0.149	4329	41323	0.105
6	0.00742	0.099	0.075	2550	48253	0.053

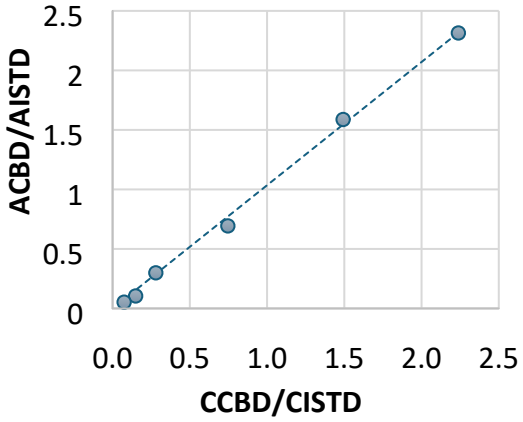

Figure S 30: Calibration curve.

The slope is equal to 1.034 with a 95% standard error of 0.017.

4.2. Results

4.2.1. Hydrogenation of Limonene

A 0.1 M solution of limonene was hydrogenated at two temperatures: 60 °C and 100 °C. The results for hydrogenation at 60 °C are reported in Table S 34. Those for the hydrogenation at 100 °C are reported in Table S 35.

Table S 34: Conversion and selectivity in the hydrogenation of limonene. Conditions: 60 °C, 20 bar, 51 s, H/S 11.2.

Entry	Collection Time	Conversion	Selectivity		
		Limonene	p-menthene	t-p-menthane	c-p-menthane
	[min]		*[%]*		
1	5	82.0	80.8	9.7	9.5
2	15	81.2	80.3	10.1	9.6
3	25	79.3	80.7	9.6	9.7
4	35	77.5	81.7	9.2	9.1
5	45	77.2	81.9	9.0	9.1

Table S 35: Conversion and selectivity in the hydrogenation of limonene. Conditions: 100 °C, 20 bar, 51 s, H/S 11.2.

Entry	Collection Time	Conversion	Selectivity		
		Limonene	p-menthene	t-p-menthane	c-p-menthane
	[min]		*[%]*		
1	5	94.7	39.8	29.6	30.6
2	15	93.1	45.0	27.1	28.0
3	25	91.9	48.2	25.8	26.0
4	35	91.1	51.8	23.7	24.5
5	45	89.9	55.6	22.0	22.4

4.2.2. Hydrogenation of Limonene in the Presence of Resorcinol

A 0.1 M solution of limonene containing 0.1 M of resorcinol was hydrogenated at two temperatures: 60 °C and 100 °C. The results for the hydrogenation at 60 °C are reported in Table S 36. Those for the hydrogenation at 100 °C are reported in Table S 37. In both cases the concentration of resorcinol remained constant throughout the investigation.

Table S 36: Conversion and selectivity in the hydrogenation of limonene with resorcinol. Conditions: 60 °C, limonene [0.1 M] + resorcinol [0.1 M], 60 °C, 20 bar, 51 s, H/S 11.2.

Entry	Collection Time	Conversion	Selectivity		
		Limonene	p-menthene	t-p-menthane	c-p-menthane
	[min]			*[%]*	
1	5	68.8	87.2	6.5	6.2
2	15	64.7	88.5	5.9	5.6
3	25	60.5	89.5	5.4	5.2
4	35	59.7	90.1	5.0	4.9
5	45	56.4	90.7	4.7	4.6

Table S 37: Conversion and selectivity in the hydrogenation of limonene with resorcinol. Conditions: limonene [0.1 M] + resorcinol [0.1 M], 100 °C, 20 bar, 51 s, H/S 11.2.

Entry	Collection Time	Conversion	Selectivity		
		Limonene	p-menthene	t-p-menthane	c-p-menthane
	[min]			*[%]*	
1	5	85.9	68.8	15.6	15.5
2	15	85.0	73.9	13.0	13.1
3	25	83.1	76.4	11.8	11.8
4	35	81.6	78.7	10.7	10.6
5	45	78.1	80.2	9.8	10.0

5. Calculations

An estimation of the impact of the internal mass transfer diffusional limitation can be obtained either with the Weisz-Prater criterium, or by calculating the diffusional Damköhler number (Da_{II}).[5,6] We opted for this second option, as it is less reliant on physical parameters that can be difficult to estimate or calculate (e.g. bed density) and it would not require the rate of reaction per volume of pellet to be computed. The reactions were considered as pseudo-first order reactions, and the Damköhler number could be computed using the following equation:

$$Da = \frac{k \cdot L^2}{D_{eff}}$$

Where k is the kinetic constant, L is the particle diameter and D_{eff} is the effective diffusion coefficient.

We made the following assumptions:

- For the calculation of the effective diffusion coefficient, we used the equation suggested by Ternan[7] and Ashraf[8]:

$$D_{eff} = D \cdot \frac{(1-\lambda)^2}{(1+P\cdot\lambda)}$$

With λ is the ratio of the molecule radius and the pore diameter and P is a fitting factor, which Ashraf set to 16.3.

- We assumed that CBD had a similar size for the molecule of CBD to the one used by Ashraf (0.5 nm), and we assumed a pore diameter of 20 nm, according to the manufacturer. This yielded a ratio equal to

$$\frac{D_{eff}}{D} = 0.68$$

- To account for errors in the diameter of the molecule and the pore size (sensitivity analysis), we tested different values of D/D_{eff} in the range of 0.4-0.7.
- The bulk diffusion coefficients of organic molecules in organic solvents were reported by different sources to assume values between $0.5\cdot10^{-9}$ and $1.5\cdot10^{-9}$ m^2s^{-1}.[6,9] An average value of 10^{-9} m^2s^{-1} was selected.
- The particle diameter was assumed in the range between 5 to 100 µm.[10]
- The kinetic constants at two temperatures (50 °C and 80 °C) as low and high points in the investigation were considered. Moreover, all three kinetic constants were considered.

The results of the calculations are reported in the table below.

Exp.	k [s^{-1}]	L [m]	Diffusion Correction factor	Deff [m^2 s^{-1}]	Da
k_1 (50°C)	0.0210	5.0E-06	4.0E-01	4.0E-10	1.3E-03
k_1 (80°C)	0.0420	5.0E-06	4.0E-01	1.0E-09	1.1E-03
k_1 (50°C)	0.0210	1.0E-04	4.0E-01	1.0E-09	2.1E-01
k_1 (80°C)	0.0420	1.0E-04	4.0E-01	1.0E-09	4.2E-01
k_2 (50°C)	0.0040	5.0E-06	4.0E-01	1.0E-09	1.0E-04
k_2 (80°C)	0.0130	5.0E-06	4.0E-01	1.0E-09	3.3E-04
k_2 (50°C)	0.0040	1.0E-04	4.0E-01	1.0E-09	4.0E-02
k_2 (80°C)	0.0130	1.0E-04	4.0E-01	1.0E-09	1.3E-01
k_3 (50°C)	0.0003	5.0E-06	4.0E-01	1.0E-09	7.5E-06
k_3 (80°C)	0.0019	5.0E-06	4.0E-01	1.0E-09	4.8E-05
k_3 (50°C)	0.0003	1.0E-04	4.0E-01	1.0E-09	3.0E-03

k_3 (80°C)	0.0019	1.0E-04	4.0E-01	1.0E-09	1.9E-02
k_1 (50°C)	0.0210	5.0E-06	7.0E-01	7.0E-10	7.5E-04
k_1 (80°C)	0.0420	5.0E-06	7.0E-01	7.0E-10	1.5E-03
k_1 (50°C)	0.0210	1.0E-04	7.0E-01	7.0E-10	3.0E-01
k_1 (80°C)	0.0420	1.0E-04	7.0E-01	7.0E-10	6.0E-01
k_2 (50°C)	0.0040	5.0E-06	7.0E-01	7.0E-10	1.4E-04
k_2 (80°C)	0.0130	5.0E-06	7.0E-01	7.0E-10	4.6E-04
k_2 (50°C)	0.0040	1.0E-04	7.0E-01	7.0E-10	5.7E-02
k_2 (80°C)	0.0130	1.0E-04	7.0E-01	7.0E-10	1.9E-01
k_3 (50°C)	0.0003	5.0E-06	7.0E-01	7.0E-10	1.1E-05
k_3 (80°C)	0.0019	5.0E-06	7.0E-01	7.0E-10	6.8E-05
k_3 (50°C)	0.0003	1.0E-04	7.0E-01	7.0E-10	4.3E-03
k_3 (80°C)	0.0019	1.0E-04	7.0E-01	7.0E-10	2.7E-02

As can be seen, Da<<1 for all the scenarios: we can confirm that the reaction is kinetically controlled.

6. Spectra

The results of the spectra were found to be in accordance with literature.[11,12,13]

6.1. GC-MS Analysis

6.1.1. CBD (1)

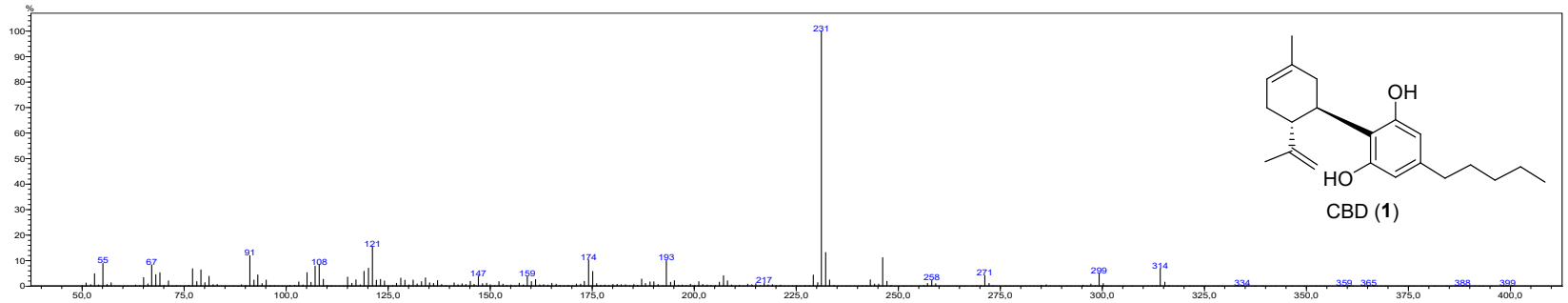

Figure S 31: Mass fragmentation of CBD.

6.1.2. H2CBD (2)

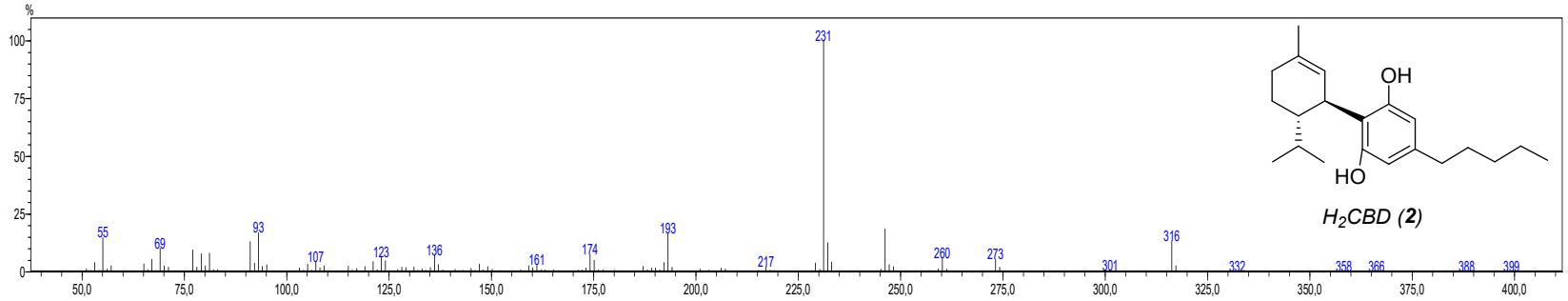

Figure S 32: Mass fragmentation of H2CBD.

6.1.3. CisH4CBD (3)

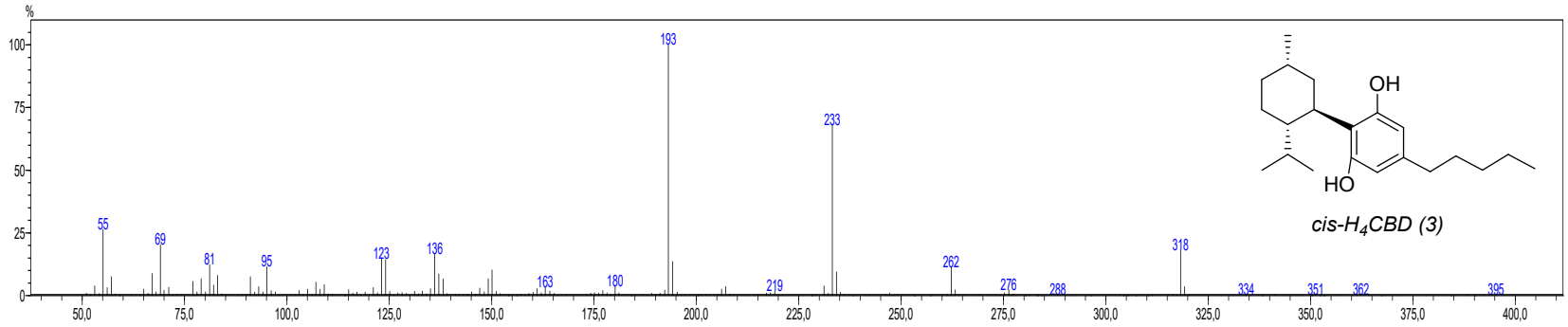

Figure S 33: Mass fragmentation of cis-H4CBD.

6.1.4. TransH4CBD (4)

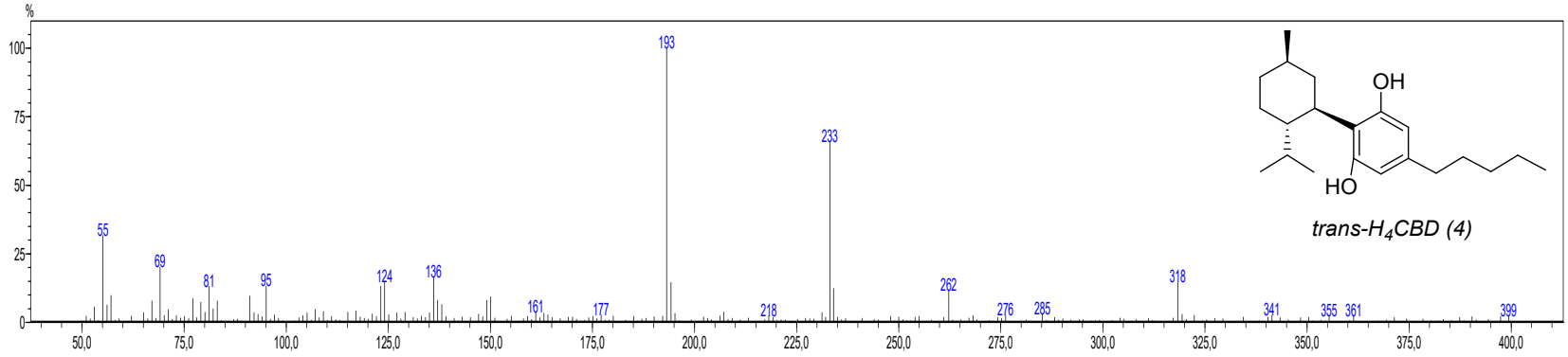

Figure S 34: Mass fragmentation of trans-H4CBD.

6.1.5. Δ^9-THC (5)

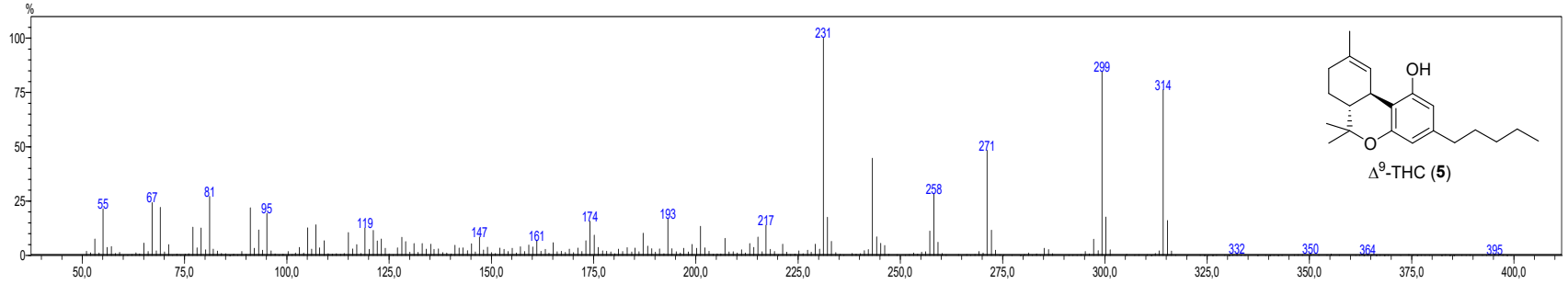

Figure S 35: Mass fragmentation of Δ^9-THC.

6.1.6. Δ^8-THC (6)

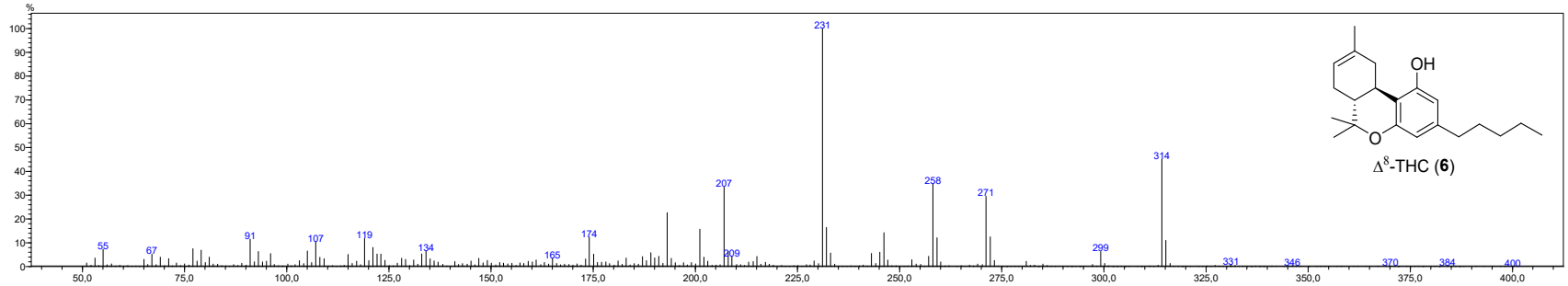

Figure S 36: Mass fragmentation of Δ^8-THC.

6.1.7. R-HHC (7)

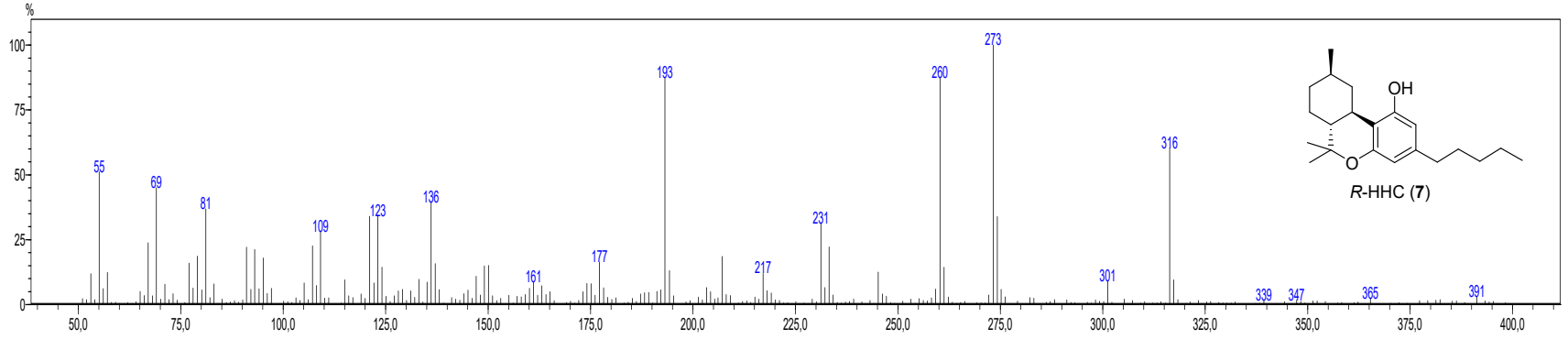

Figure S 37: Mass fragmentation of R-HHC.

6.1.8. S-HHC (8)

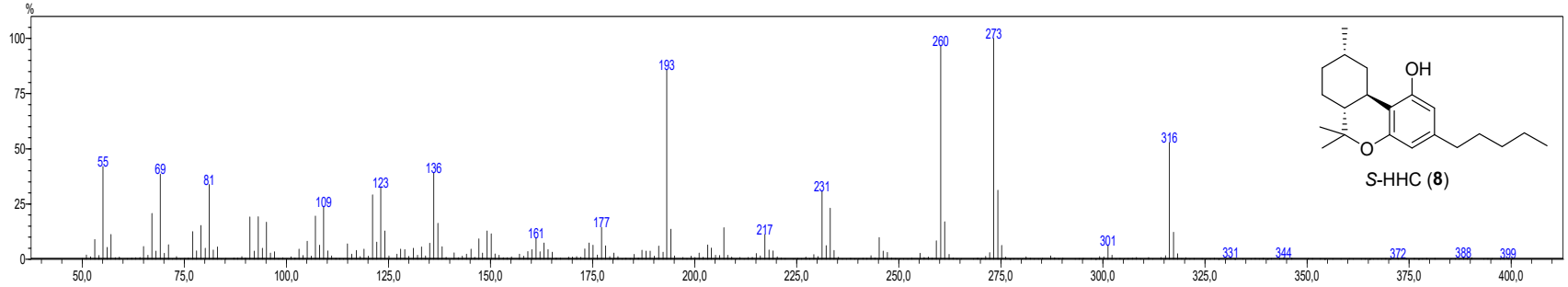

Figure S 38: Mass fragmentation of S-HHC.

6.2. NMR Spectra

6.2.1. Cannabidiol (CBD)

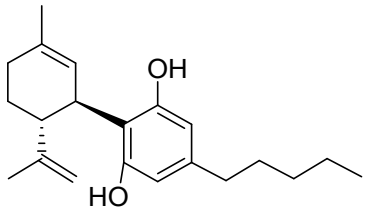

CBD (**1**)

White Powder

^{1}H NMR (300 MHz, Acetonitrile-d3) δ 6.13 (s, 1H), 5.28 (tq, J = 2.5, 1.2 Hz, 1H), 4.46 (ddt, J = 3.6, 1.9, 1.1 Hz, 1H), 3.89 (ddp, J = 11.2, 4.7, 2.4 Hz, 1H), 2.79 – 2.65 (m, 1H), 2.39 (t, 1H), 2.29 – 2.13 (m, 1H), 2.05 (q, J = 3.3 Hz, 0H), 1.99 (q, J = 3.3 Hz, 0H), 1.94 (p, J = 2.5 Hz, 0H), 1.79 – 1.71 (m, 1H), 1.70 (dd, J = 2.8, 1.5 Hz, 2H), 1.64 (t, J = 1.1 Hz, 2H), 1.59 – 1.47 (m, 1H), 1.40 – 1.21 (m, 2H), 0.89 (t, J = 6.9 Hz, 2H).

^{13}C NMR (75 MHz, CD_3CN) δ 149.1, 142.2, 135.8, 124.9, 114.2, 109.7, 45.4, 35.8, 35.0, 31.3, 30.6, 30.2, 29.1, 22.7, 22.3, 18.4, 13.4, 1.2, 0.9, 0.6, 0.4, 0.1, −0.2, −0.5.

6.2.2. Dihydro Cannabidiol (H2CBD)

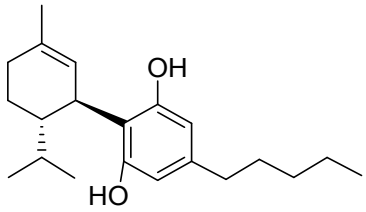

H_2CBD (**2**)

Colorless oil

^{1}H NMR (300 MHz. Acetonitrile-d3) δ 6.17 (s, 1H), 5.32 (s, 0H), 3.77 (d, J = 14.1 Hz, 0H), 2.48 – 2.34 (m, 1H), 2.17 (s, 1H), 2.15 – 2.00 (m, 1H), 1.71 (s, 2H), 1.61 – 1.42 (m, 2H), 1.40 – 1.25 (m, 3H), 0.89 (t, J = 6.9 Hz, 1H), 0.83 (d, J = 3.1 Hz, 2H), 0.81 (d, J = 2.9 Hz, 1H).

^{13}C NMR (75 MHz. CD3CN) δ 181.4, 157.0, 143.4, 138.4, 126.0, 115.2, 43.9, 36.3, 36.0, 32.3, 31.6, 31.3, 28.9, 23.6, 23.2, 23.2, 21.9, 16.6, 14.3.

6.2.3. Tetrahydro Cannabidiol (H4CBD)

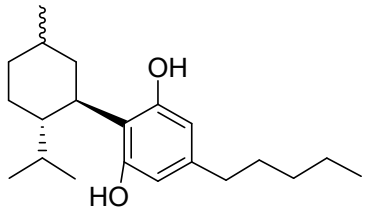

H_4CBD (3,4)

Yellow Oil

^{1}H NMR (300 MHz. Acetonitrile-d3) δ 6.54 (s, 1H), 6.48 (s, 1H), 6.15 (d, J = 1.5 Hz, 1H), 6.09 (d, J = 1.4 Hz, 1H), 2.98 (td, J = 11.6, 3.3 Hz, 1H), 2.45 – 2.34 (m, 3H), 2.21 (s, 2H), 2.12 (ddd, J = 11.4, 8.6, 2.9 Hz, 2H), 1.80 – 1.24 (m, 16H), 1.10 – 0.96 (m, 3H), 0.95 – 0.84 (m, 7H), 0.81 (d, J = 7.0 Hz, 3H), 0.67 (s, 2H).

^{13}C NMR (75 MHz. CD3CN) δ 157.5, 156.2, 142.4, 116.2, 108.8, 108.1, 45.4, 44.5, 40.7, 38.8, 37.4, 36.4, 35.9, 34.4, 33.0, 32.6, 32.3, 31.6, 29.6, 29.4, 26.0, 23.2, 22.9, 21.9, 21.7, 20.1, 18.4, 16.0, 14.3.

6.2.4. Δ^9-Tetrahydro Cannabinol (Δ_9-THC)

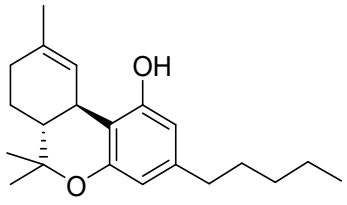

Δ^9-THC (5)

Colorless oil

^{1}H NMR (300 MHz. Acetonitrile-d3) δ 6.79 (s. 1H). 6.32 (h. J = 1.7 Hz. 1H). 6.17 (d. J = 1.7 Hz. 1H). 6.10 (d. J = 1.7 Hz. 1H). 3.13 (dq. J = 10.5. 2.5 Hz. 1H), 2.46 – 2.36 (m. 2H). 2.18 (s, 1H), 2.16 (s, 0H), 1.91 (dddd, J = 16.1, 5.3, 3.6, 1.6 Hz, 1H), 1.64 (dq, J = 2.3, 1.0 Hz, 3H), 1.61 – 1.48 (m, 3H), 1.35 (s, 4H), 1.34 – 1.24 (m, 2H), 1.20 (t, J = 7.1 Hz, 3H), 1.02 (s, 3H).

^{13}C NMR (75 MHz. CD3CN) δ 171.6, 156.5, 155.7, 143.5, 134.2, 125.2, 110.0, 109.9, 108.2, 77.7, 60.9, 46.8, 36.0, 34.5, 32.2, 31.8, 31.6, 27.8, 25.7, 23.5, 23.2, 21.1, 19.5, 14.5, 14.3, 2.1, 1.8, 1.6, 1.3, 1.0, 0.7, 0.5.

6.2.5. Δ_8-Tetrahydro Cannabinol (Δ_8-THC)

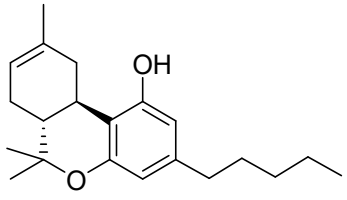

Δ^8-THC (6)

Colorless oil

^{1}H NMR (300 MHz. Acetonitrile-d3) δ 6.17 (d, J = 1.7 Hz, 1H), 6.11 (d, J = 1.7 Hz, 1H), 5.48 – 5.37 (m, 1H), 3.29 – 3.14 (m, 1H), 2.60 (td, J = 11.1, 4.7 Hz, 1H), 2.46 – 2.37 (m, 2H), 2.33 (s, 2H), 2.20 (s, 3H), 1.84 (ddt, J = 14.1, 4.3, 2.1 Hz, 1H), 1.73 – 1.62 (m, J = 3.7 Hz, 4H), 1.54 (dq, J = 9.7, 7.2 Hz, 2H), 1.39 – 1.23 (m, 8H), 1.03 (s, 3H), 0.89 (t, J = 6.9 Hz, 3H),

^{13}C NMR (75 MHz. CD3CN) δ 157.0, 155.7, 143.5, 135.3, 120.5, 111.4, 109.9, 108.3, 77.1, 46.0, 36.7, 36.0, 32.5, 32.2, 31.6, 28.5, 27.8, 23.6, 23.2, 18.7, 14.3.

6.2.6. Hexahydro Cannabinol (HHC)

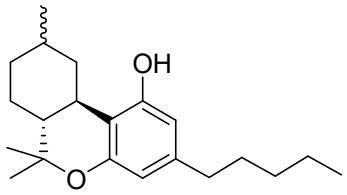

HHC (7,8)

Pale Yellow Oil

^{1}H NMR (300 MHz. Acetonitrile-d3) δ 6.71 (s, 1H), 6.67 (s, 0H), 6.12 (t, J = 2.2 Hz, 2H), 6.07 (t, J = 1.6 Hz, 2H), 3.12 – 3.00 (m, 1H, R-HHC), 2.99 – 2.89 (m, 1H, S-HHC), 2.62 (td, J = 11.2, 3.0 Hz, 1H), 2.39 (dd, J = 9.2, 6.2 Hz, 4H), 2.16 (s, 2H), 1.83 (dt, J = 11.2, 2.3 Hz, 2H), 1.69 – 1.57 (m, 0H), 1.53 (ddd, J = 7.8, 6.4, 1.5 Hz, 2H), 1.45 – 1.33 (m, 3H), 1.33 – 1.26 (m, 9H), 1.20 (t, J = 7.1 Hz, 1H), 1.10 (d, J = 7.2 Hz, 2H), 1.01 (d, J = 7.3 Hz, 5H), 0.95 – 0.84 (m, 8H).

^{13}C NMR (75 MHz. CD3CN) δ 157.0, 156.1, 155.8, 143.3, 118.3, 111.4, 111.2, 109.8, 108.2, 77.4, 77.3, 51.0, 50.1, 39.7, 36.7, 36.3, 35.9, 33.6, 33.0, 32.2, 31.6, 30.2, 28.8, 28.7, 28.0, 27.9, 23.7, 23.2, 22.9, 19.3, 19.2, 19.0, 14.5, 14.3, 2.1, 1.8, 1.6, 1.3, 1.0, 0.7, 0.5.

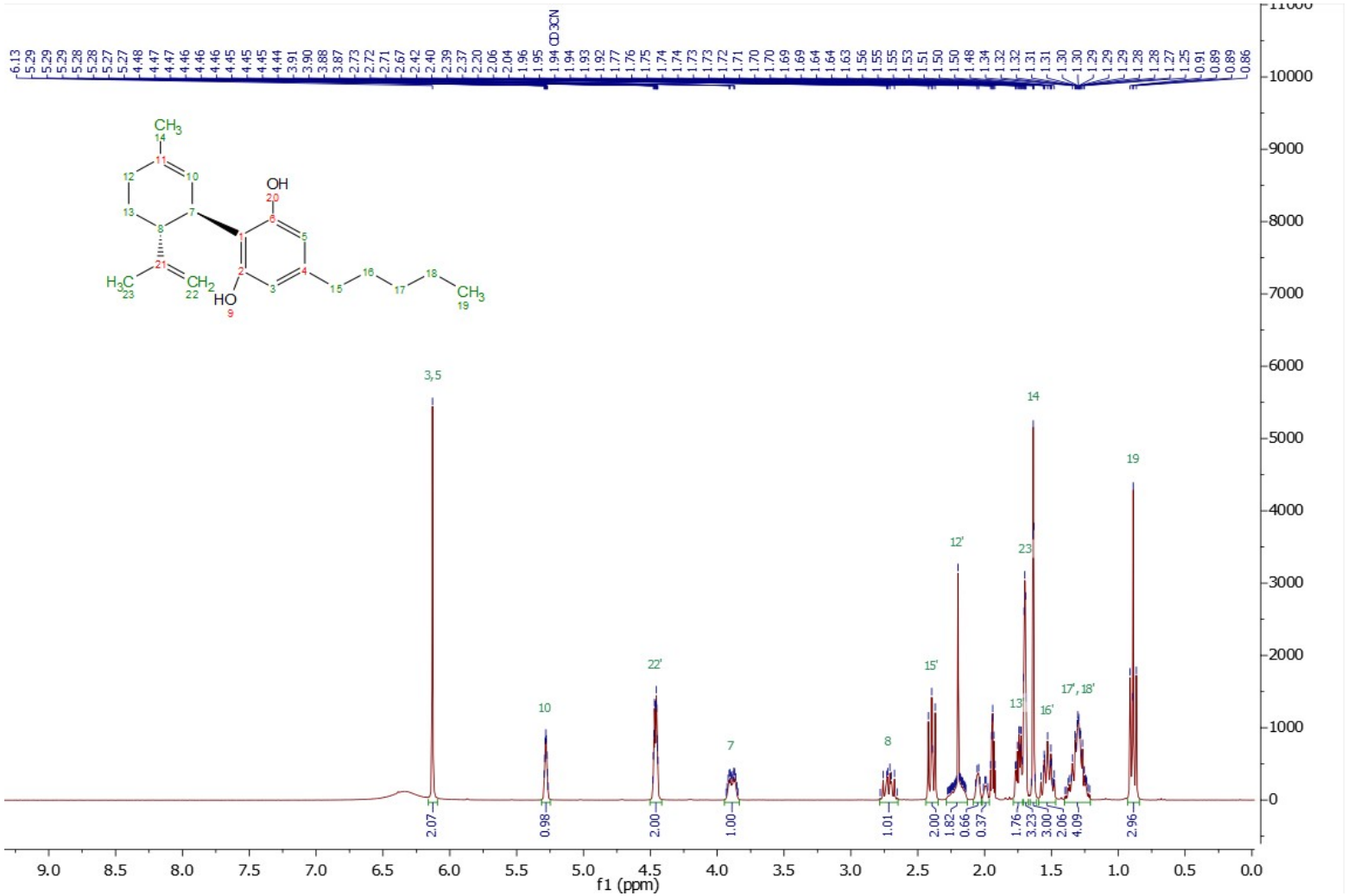

*Figure S 39: ^{1}H NMR spectrum of CBD (**1**).*

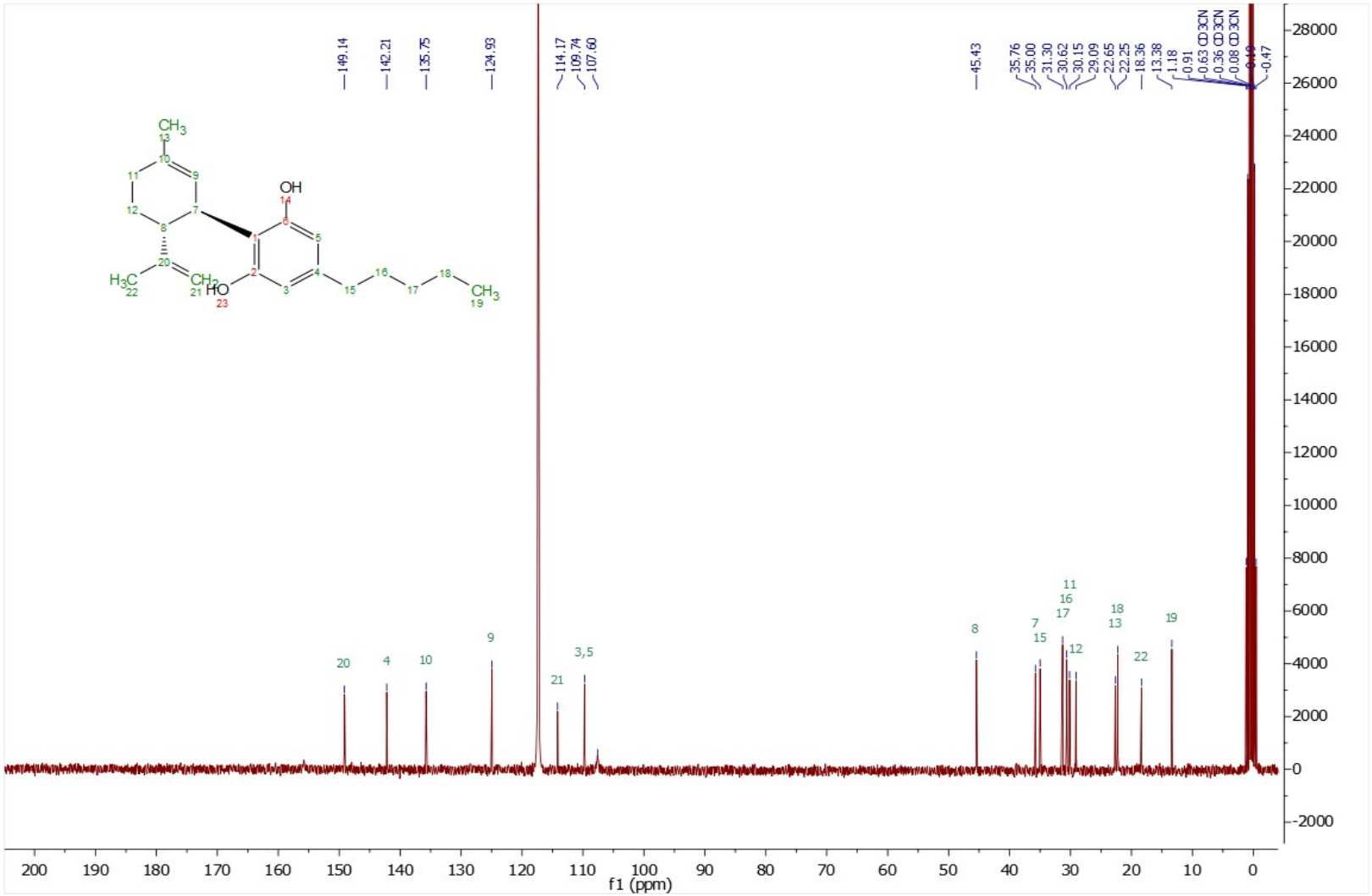

*Figure S 40: ^{13}C NMR spectrum of CBD (**1**).*

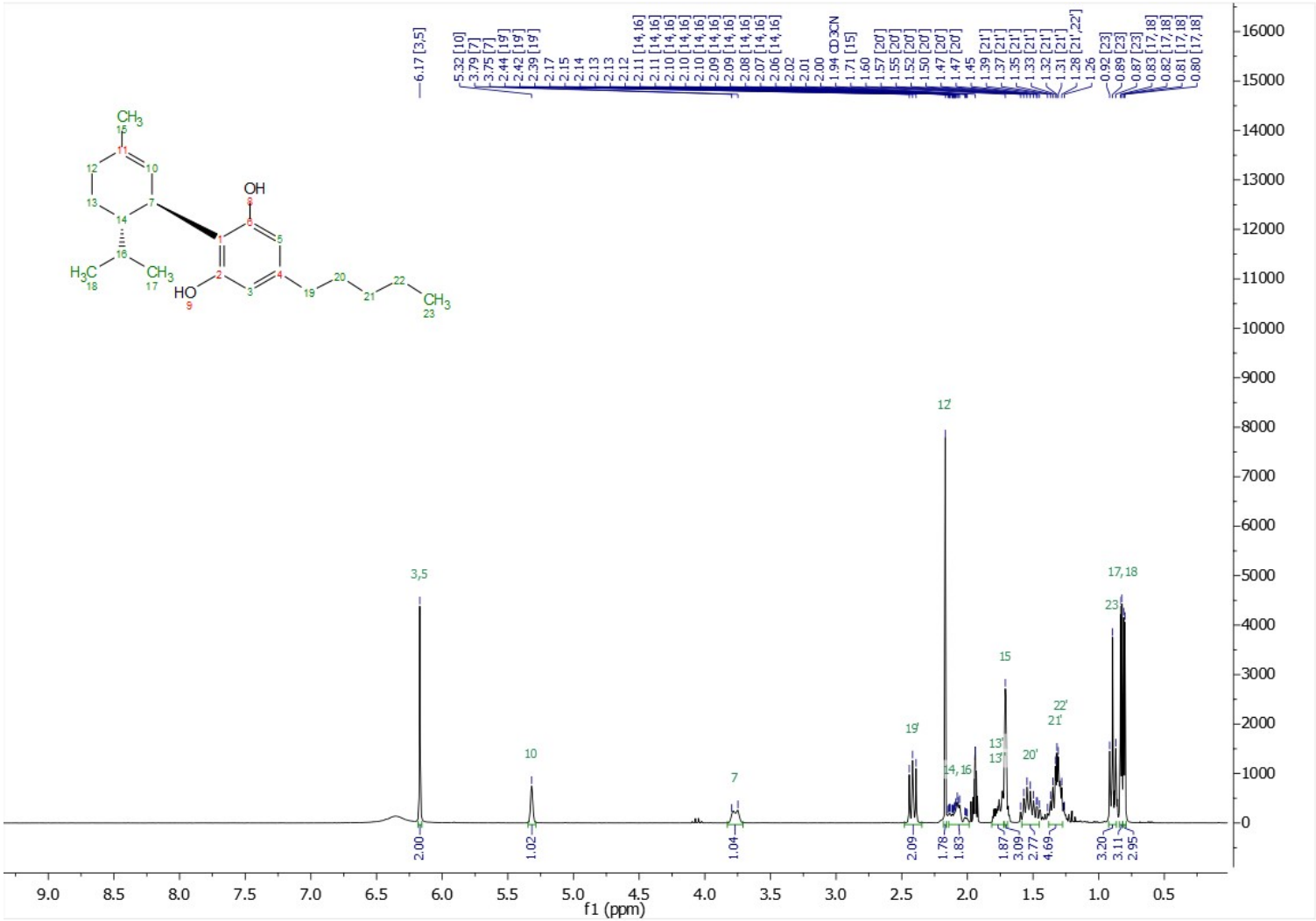

*Figure S 41: ^{1}H NMR spectrum of H2CBD (**2**).*

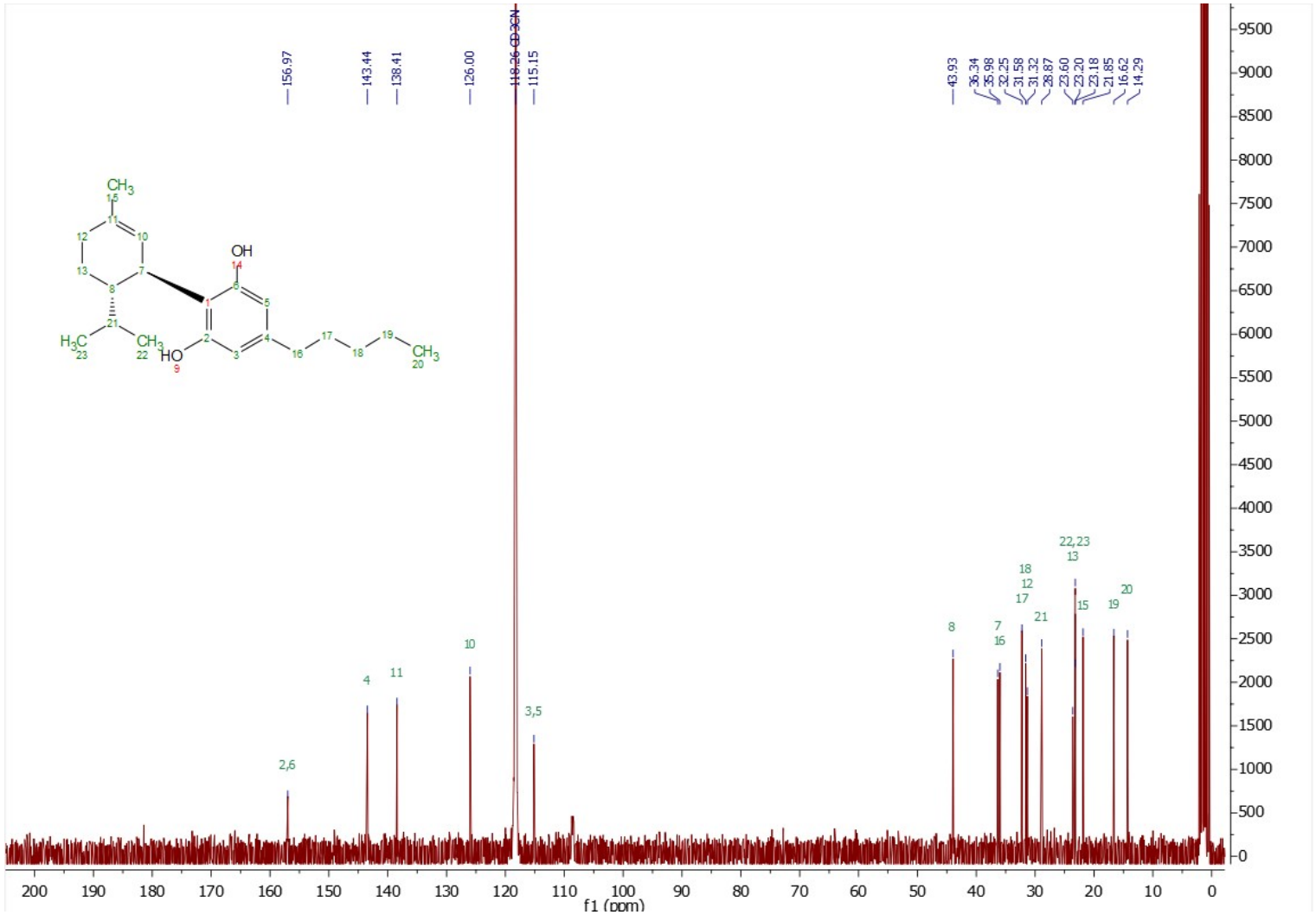

*Figure S 42: ^{13}C NMR spectrum of H2CBD (**2**).*

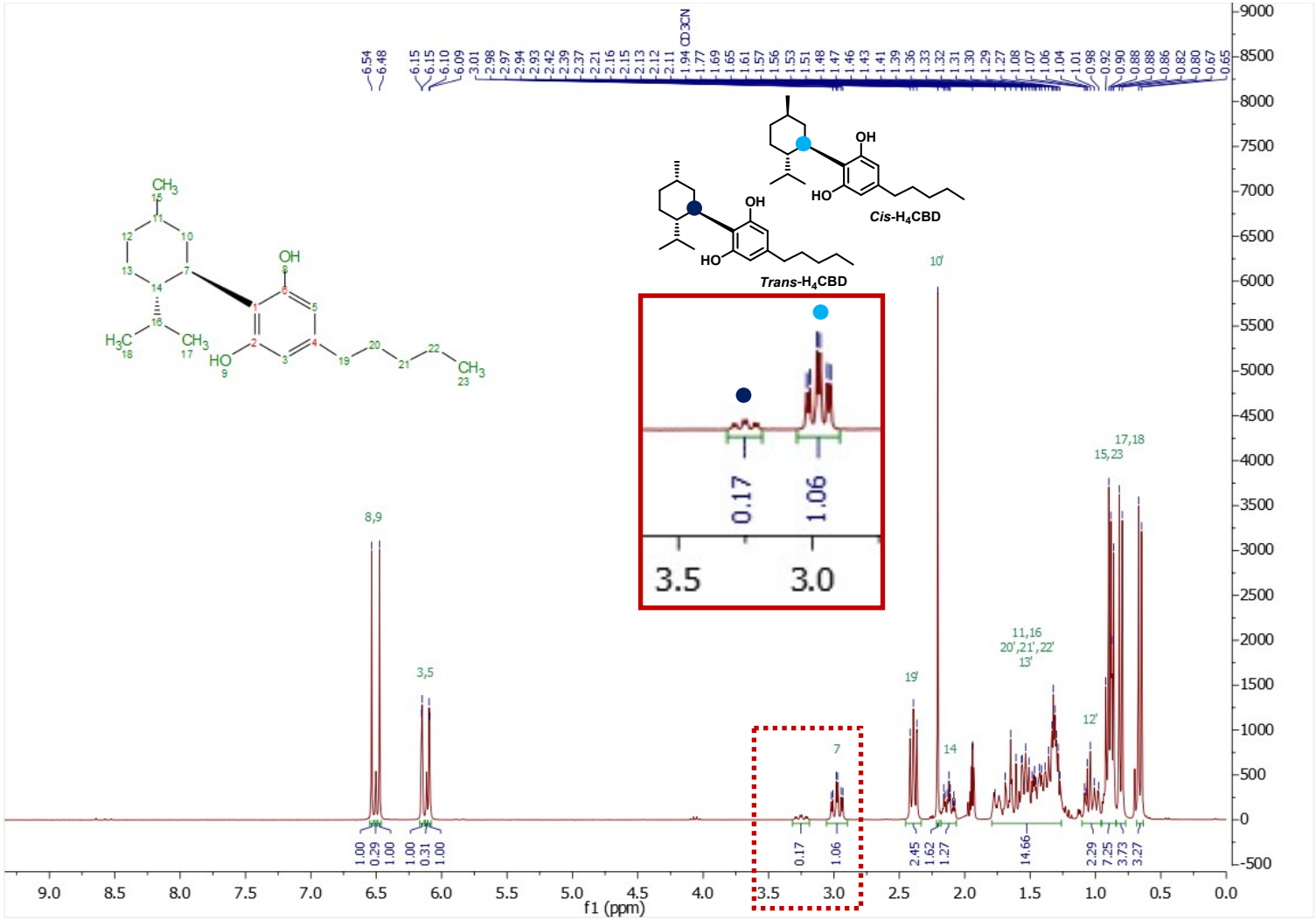

*Figure S 43: ^{1}H NMR spectrum of H4CBD diastereomers mixture (**3**, **4**).*

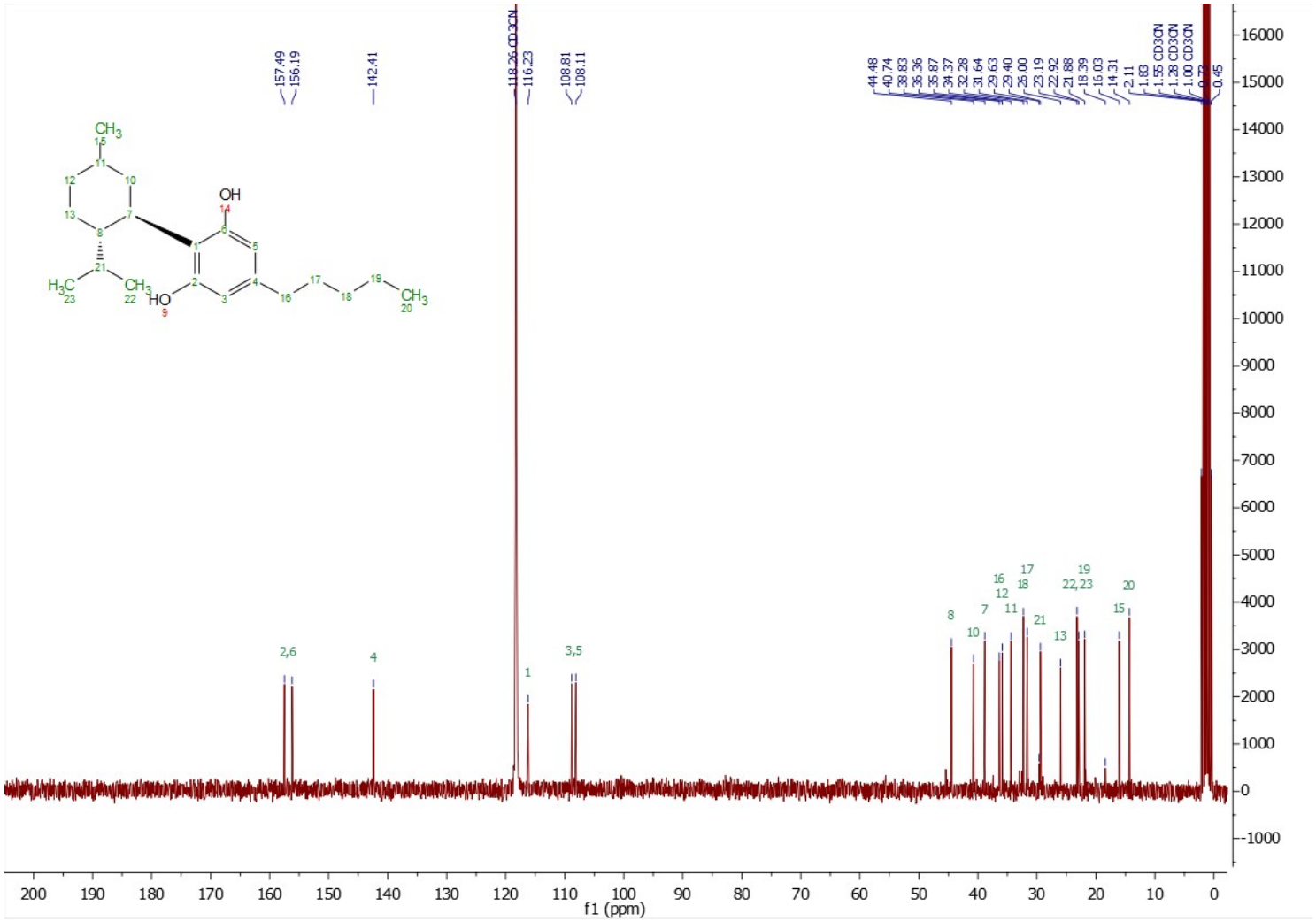

*Figure S 44: ^{13}C NMR spectrum of H4CBD diastereomers (**3**, **4**).*

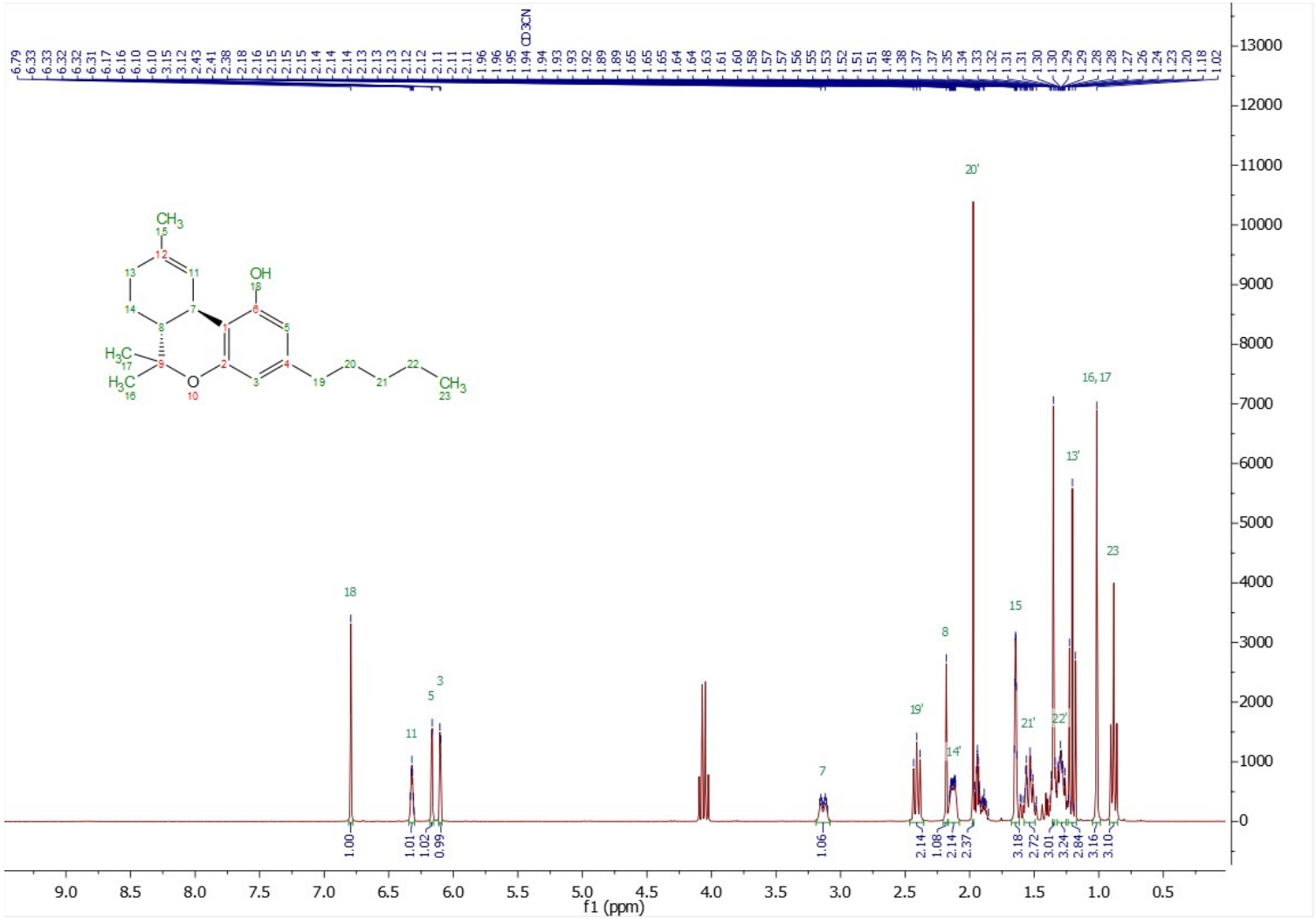

*Figure S 45: ^{1}H NMR spectrum of Δ^{9}-THC (**5**).*

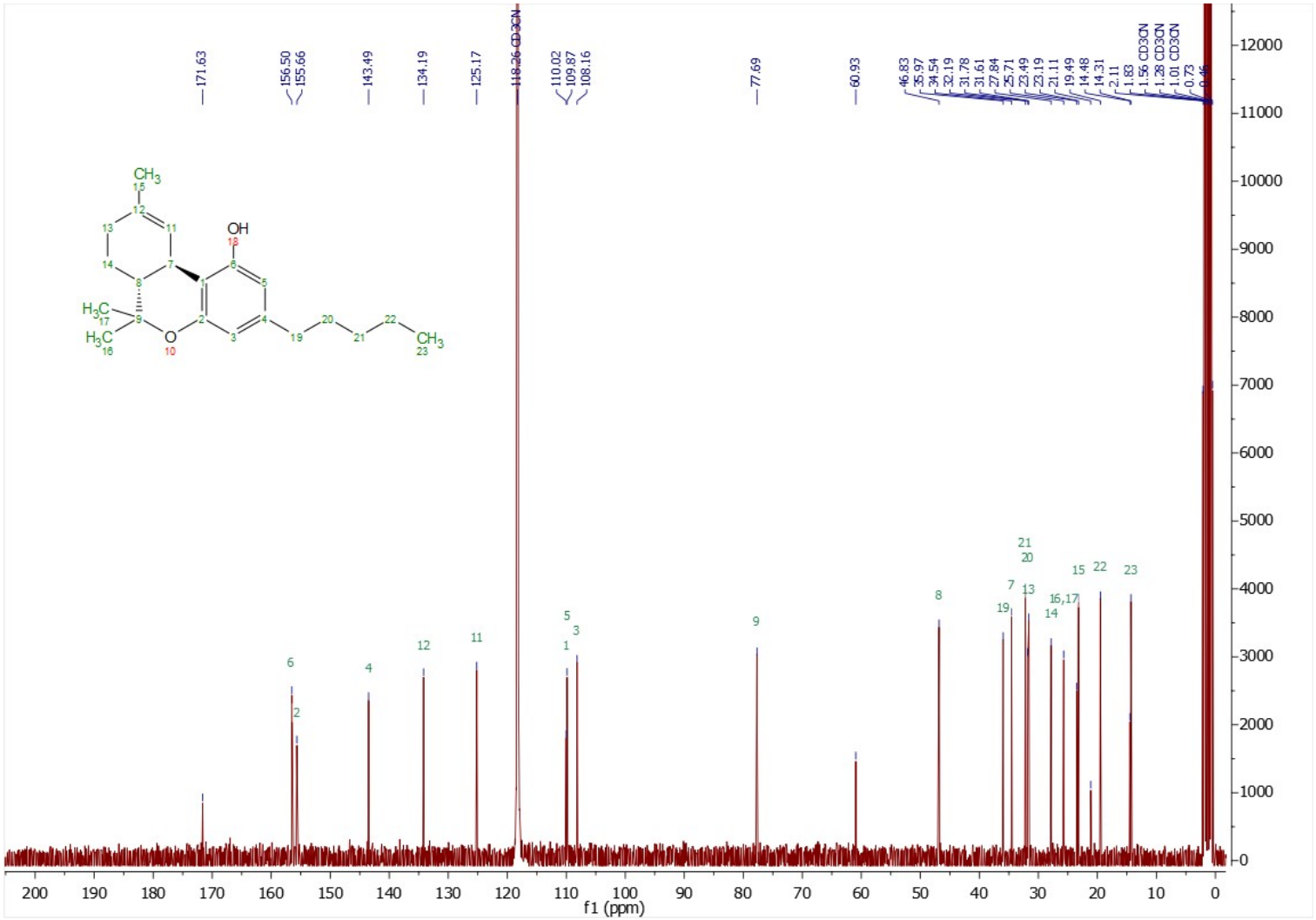

*Figure S 46: ^{13}C NMR spectrum of Δ^9-THC (**5**).*

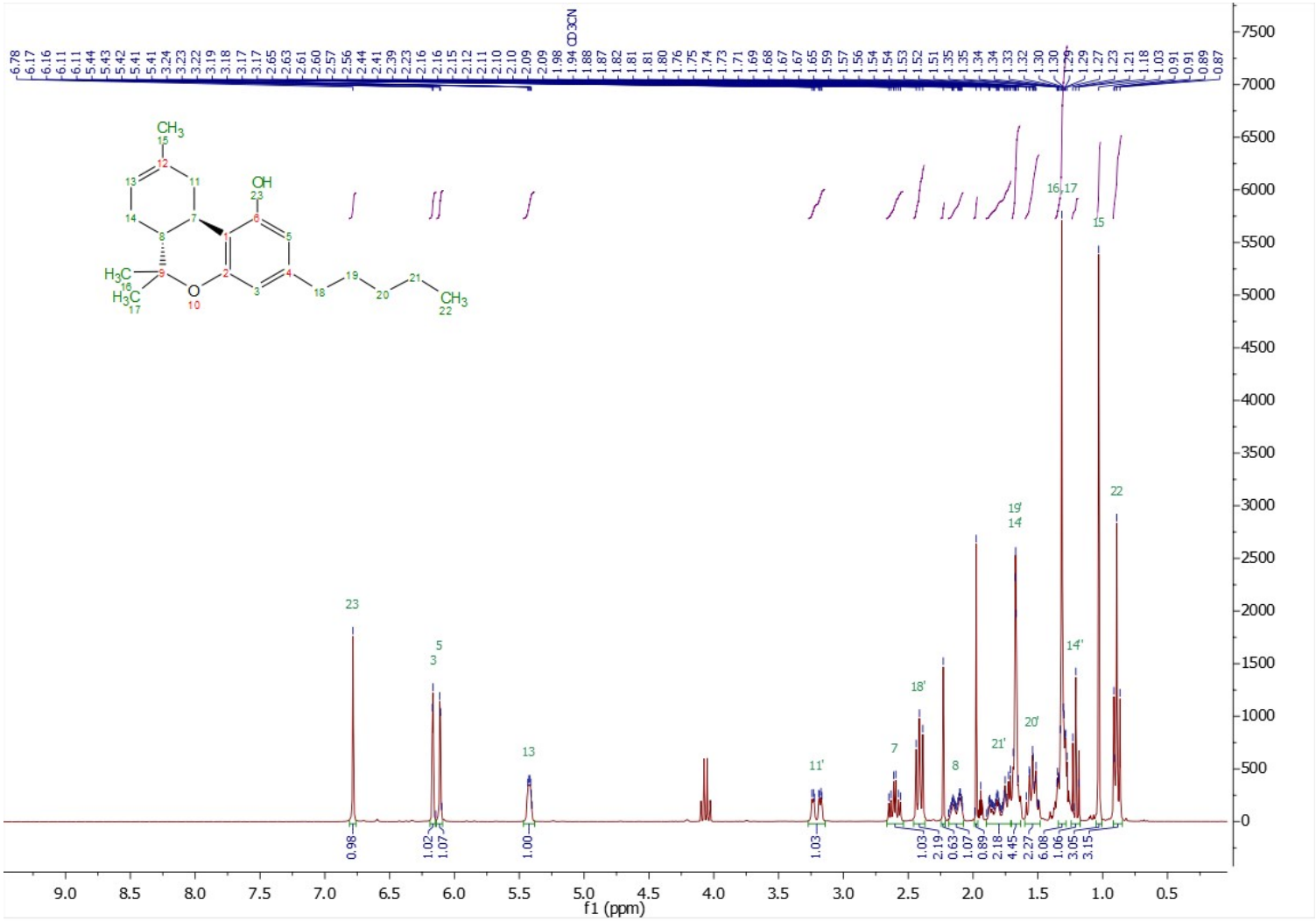

*Figure S 47: ^{1}H NMR of Δ^{8}-THC (**6**).*

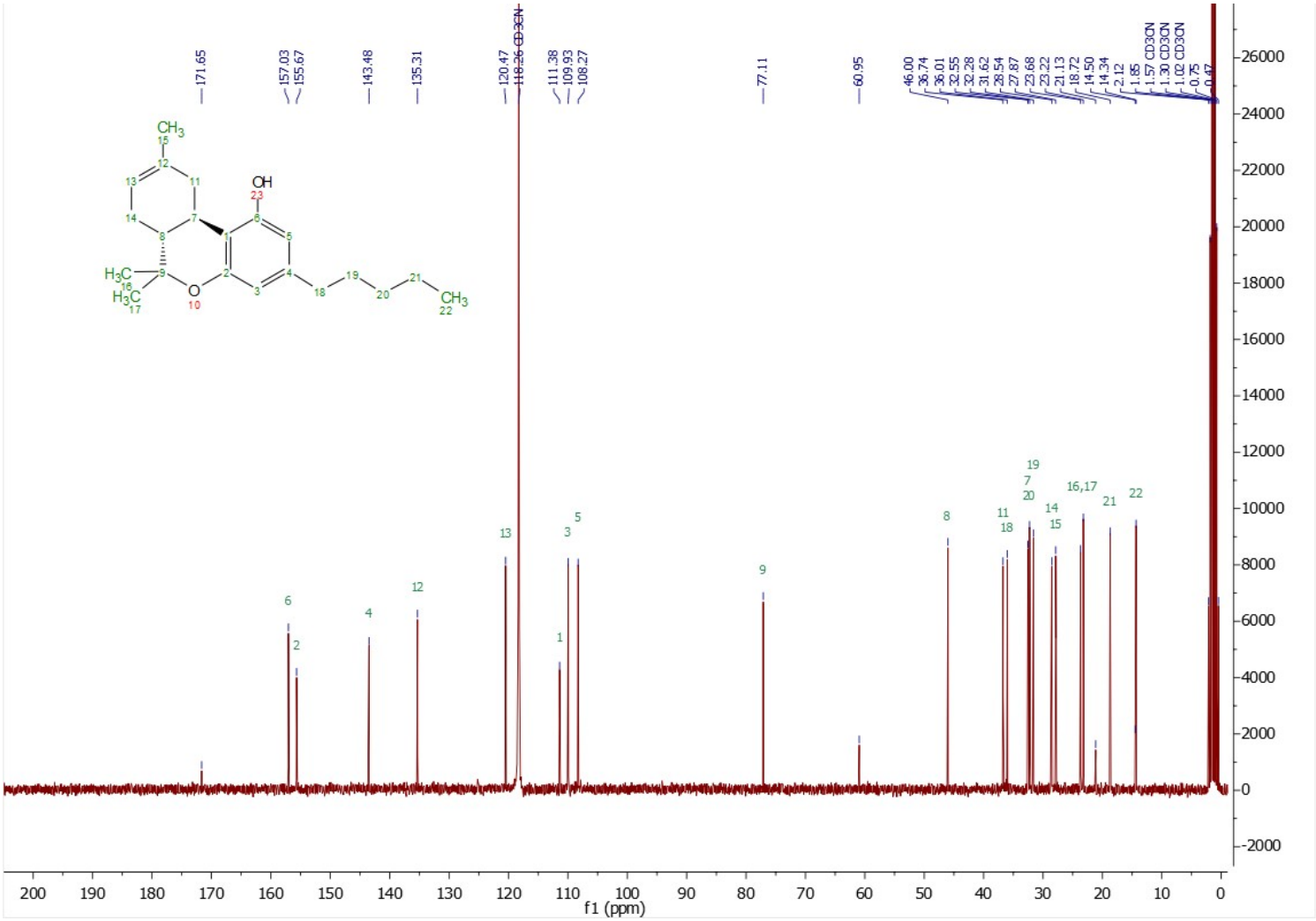

*Figure S 48: ^{13}C NMR of Δ^8-THC (**6**).*

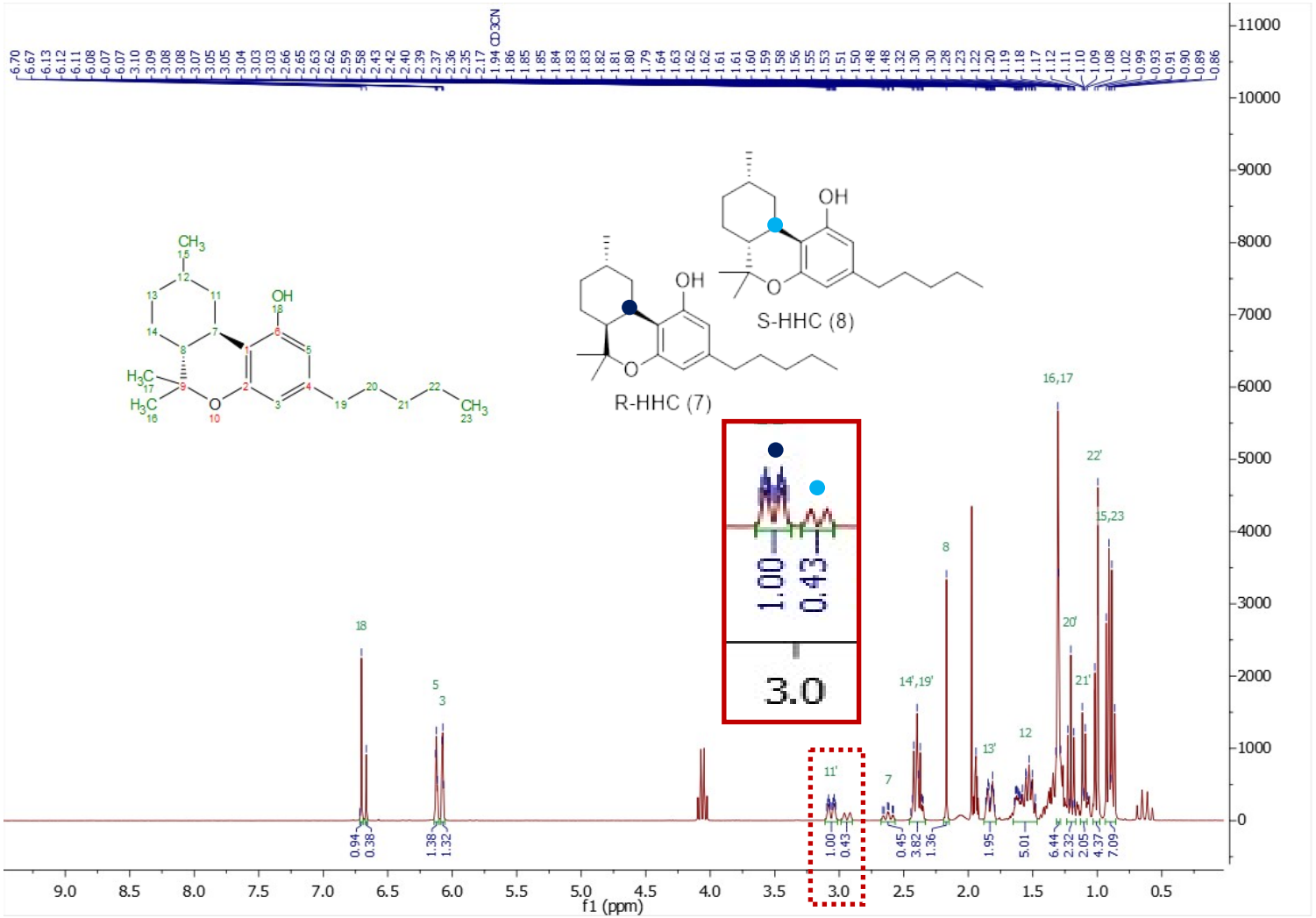

*Figure S 49: ^{1}H NMR spectrum of HHC diastereomers (**7**, **8**).*

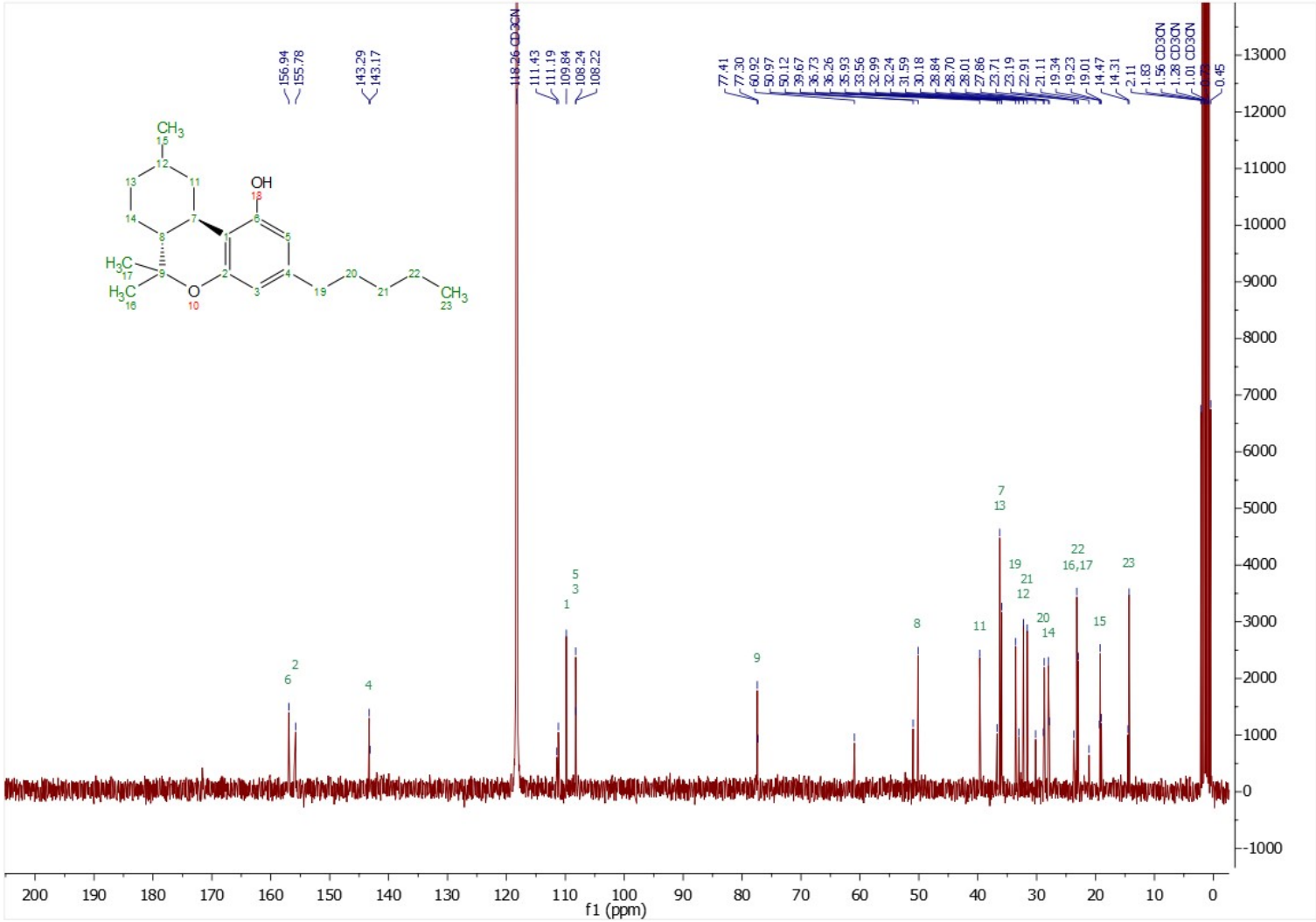

*Figure S 50: ^{13}C NMR spectrum of HHC diastereomers (**7**, **8**).*

7. References

[1] R. Lebl, S. Bachmann, P. Tosatti, J. Sedelmeier, K. Püntener, J. D. Williams, C. O. Kappe, Catalytic Static Mixer-Enabled Hydrogenation of a Key Fenebrutinib Intermediate: Real-time Analysis for a Stable and Scalable Process *Org. Process Res. Dev.,* **2021**, 25, 1988

[2] R. Lebl, Y. Zhu, D. Ng, C.H. Hornung, D. Cantillo, C.O. Kappe, Scalable continuous flow hydrogenations using Pd/Al_2O_3-coated rectangular cross-section 3D-printed static mixers, *Catal. Today*, **2022**, 383, 55

[3] G.R.B. Webster, L.P. Sarna, R. Mechoulam, US20040143126A1, **2004**

[4] G. Chure, J. Cremer, Hplc-py: A Python Utility for Rapid Quantification of Complex Chemical Chromatograms, *J. Open Source Softw.*, **2024**, 9(94), 6270

[5] O. Levenspeil, Chemical Reaction Engineering, John Wiley & Sons, New York, 1998

[6] K. D. Nagy, B. Shen, T. F. Jamison and K. F. Jensen. Mixing and Dispersion in Small-Scale Flow Systems. *Org. Process Res. Dev.* **2012**, 16, 976–981

[7] M. Ternan, The Diffusion of Liquids in Pores. *Can. J. Chem. Eng.* **1987**, 65, 1987, 245-249

[8] M.A. Ashraf, J. Tan, M.G. Davidson, S. Bull, M. Hutchby, D. Mattia and P. Plucinski, Continuous-flow liquid-phase dehydrogenation of 1,4-cyclohexanedione in a structured multichannel reactor. *React. Chem. Eng*., **2019**, 4, 27-40

[9] E.E. Hills, M.H. Abraham, A. Hersey and C.D. Bevan, Diffusion coefficients in ethanol and in water at 298 K: Linear free energy relationships. *Fluid Ph. Equilib.* **2011**, 303, 45–55.

[10] Stanford Advanced Materials, https://www.samaterials.com/palladium/964-palladium-on-alumina-pdal2o3.html Received 7th March 2025.

[11] P. Seccamani, C. Franco, S. Protti, A. Porta, A. Profumo, D. Caprioglio, S. Salamone, B. Mannucci, D. Merli, Photochemistry of Cannabidiol (CBD) Revised. A combined Preparative and Spectrometric Investigation, *J. Nat. Prod.*, **2021**, 84, 2858.

[12] P.S. Cham, Deepika, R. Bhat, D. Raina, D. Manhas, P. Kotwal, D.P. Mindala, N.Pandey, A. Ghosh, S. Saran, U. Nandi, I. Ali Khan, P.P. Singh, Exploring the antibacterial potential of semisynthetic phytocannabinoid: tetrahydrocannabidiol (THCBD) as a potential antibacterial agent against sensitive and resistant strains of Staphylococcus aureus, *ACS Infect. Dis.*, **2024**, 10, 64

[13] A. Collins, G. Ramirez, T. Tesfatsion, K.P. Ray, S. Caudill, W. Cruces, Synthesis and Characterization of the Diastereomers of HHC and H4CBD, *Nat. Prod. Communications*, **2023**, 18, 3, 1.